

TKI PRISMA II

Overview report



TKI PRISMA II
Overview report

Auteur(s)
Lynrd de Wit
Floris van Rees

TKI PRISMA II
Overview report

Client	TKI consortium of Havenbedrijf Rotterdam N.V. (Port of Rotterdam), Rijkswaterstaat, Van der Kamp, Port of Hamburg, TU Delft, Deltares
Contact	E. Hupkes, G. Kant, A. van Hassent (PoR), S. Rockx, R. Lievens, K. Nipius (RWS), H. Veerman (vdKamp), N. Ohle (PoH), A. Kirichek, G. Keetels (TUD), L. de Wit, F. van Rees, G. Santinelli (Deltares)
Reference	
Keywords	Maintenance dredging, sustainable, water injection dredging, sailing through mud, port sedimentation, data science

Document control

Version	1.0
Date	18-11-2022
Project nr.	11206938-000
Document ID	11206938-000-ZKS-0002
Pages	45
Classification	
Status	definitief

Author(s)

Lynyrd de Wit		
Floris van Rees		

Doc. version	Author	Reviewer	Approver	Publish
1.0	Lynyrd de Wit	Thijs van Kessel	Toon Segeren	
	Floris van Rees			

Summary

This report provides an overview of all activities carried out within project TKI Prisma 2. PRISMA stands for "PRogramma Innovatief Sediment Management". Its aim is to reduce maintenance dredging costs and emissions (a.o. GHG emissions). Within TKI Prisma 2 research has been carried out in three work packages:

1. Water Injection Dredging (WID) monitoring and modelling
2. Large scale experiments in water-soil flume Deltares
3. Data science for optimizing dredging

This overview report gives a brief summary of key findings of each component and directs an interested reader towards the underlying reports, memos and presentations for more information. The main progress achieved within the different work packages is summarized below together with the knowledge gaps that are answered.

Work package 1

A brief two-day field monitoring campaign during and after performing WID in the Calandkanaal area was carried out to compare the vertical turbidity profiles during and after WID. The campaign consisted of a limited number of measurements and some transects had different hydrodynamic conditions, which hinders the interpretation. However, already this brief campaign confirms the common experience on the potential environment impact of WID: the increase of turbidity caused by WID, when applied well, remains in the lower parts of the water column. This campaign helps to fill the knowledge gap on the potential environmental impact of WID in the PoR.

To be able to simulate WID actions in the PoR area the COSUMO (Coupled Subgrid Models) coupling module is extended. It can now couple near-field detailed CFD (Computational Fluid Dynamics) simulations of WID actions to the Delft3D sediment transport model of the entire PoR area. In this manner it is possible to simulate the influence of WID on the sediment distribution on port scale, while incorporating local details of WID like the density driven flow behaviour and local mixing.

A rheological model is implemented in the CFD model TUDflow3D to capture the non-Newtonian behaviour of a fluid mud layer generated by WID. The implementation is verified by analytical benchmark solutions and WID experimental measurements. With this implementation even more flow details of WID actions can be simulated. This results in more accurate understanding of WID dredging.

Sediment transport simulations of the PoR area of different periods of the year and with/without 1m sea level rise (SLR) are compared to investigate the robustness of the outcomes and potential impacts of SLR on sedimentation. 1m SLR as simulated in a schematised way impacts the hydrodynamics, salt intrusion, influence of wave-induced resuspension at the North Sea and subsequently the sedimentation in the port area in a noticeable manner. Especially for port basins near the location of the estuary turbidity maximum at the end of the intrusion of the salt wedge, the sedimentation is altered by SLR. Sedimentation in the Botlek (-14%) and Europoort (-22%) slightly decreases in the scenario with SLR, whereas sedimentation increases in the basins near the new location of the salt wedge (i.e. Pernis, Waalhaven, Fruithaven, approx.+15%). A comparison of the different periods shows that the sedimentation in sub-basins of the Port of Rotterdam area vary strongly (up to +49% and -77%) between the different periods, but the total sedimentation in the entire port area varies less (+/- 22%). Hence, the overall sedimentation results obtained with the Delft3D sediment transport model for the

reference period are robust and can be used to give an indication of the expected year-round sedimentation.

Work package 2

In the large-scale sailing through mud (STM) experiment in the water-soil flume at Deltares the resistance force of an object pulled through real fluid mud from the PoR has been measured. Tests are performed for different pulling velocities (0.25-1 m/s) and different mud strengths (Bingham yield stress of 9, 17 and 21 Pa). The relation between mud mixture density and strength is established for different mud types in the PoR, including a rheological and thixotropic characterization of the mud. The obtained resistance forces are used for validation of a CFD model at TUD/Marin for ship sailing through mud. This will help to fill the knowledge gap on the ship response when sailing through mud. It is an important step to get the concept of a nautical bottom based on rheological properties accepted for use inside ports.

Large-scale WID experiments have been carried out in the water-soil flume at Deltares. Real mud from the PoR was used with Bingham yield stresses between 80 Pa and 237 Pa. Detailed density and velocity profile measurements are conducted inside the fluid mud layer generated by WID in the experiment. They are used for CFD model validation. Flow velocities inside the WID density current range between 0-0.6 m/s at the ramp with densities up to 1.15 g/cm³ and a height of 0.1-0.4 m. An interesting observation is that subsequent WID runs on the same bed give extra jet penetration compared to the previous run with similar settings. It is not fully understood yet what causes this observed phenomenon. The experiments give extra insight in the optimal SOD (stand-off distance) of a WID jet nozzle bar: when maximum penetration depth into the fluid mud bed is desired then zero SOD should be used; and when maximum horizontal transport is desired a SOD outside the flow development region of the jets (tested is ~12x nozzle diameter) should be used.

Work package 3

In work package 3 a data-driven decision support tool for maintenance dredging operations is developed. Trips in two areas with distinct sediment types (Botlek muddy sediment and Maassluis sandy sediment) are analysed. On-board dredging data was combined with bathymetric surveys and compliance with NGD (Nautical Guaranteed Depth). The results show that more than 70% of the locations along the dredging trajectory were already complying with the NGD before and after in Maassluis and Botlek. According to PoR this is preventive dredging. In Maassluis cases (mostly sandy channel bed), less than 5% of locations along the dredging trajectories were categorized as not complying before and after the dredging activity. This number is much lower than in the two Botlek cases (mostly silty channel) where it was found to be 13 and 26%. The dredging desktop data in the four cases show that locations that did not comply with NGD (before and after dredging) show a high density of sediment-water mixture inside the suction pipe. Apparently, at spots which do not comply before and after dredging, the dredging efficiency is not the problem, but simply more dredging trails on those spots are needed.

A list of all detail reports, memos, data sets, graduation reports and publications from TKI Prisma 2 is provided in Section 5.

Contents

	Summary	4
	List of abbreviations	8
1	Introduction	9
1.1	Background	9
1.1.1	Introduction	9
1.1.2	Water injection dredging	10
1.1.3	Nautical bottom based on rheological properties	10
1.2	Objectives	11
1.3	Outline	12
2	WP1: Water Injection Dredging monitoring and modelling	13
2.1	Introduction	13
2.2	Field monitoring WID Calandkanaal area	13
2.3	COSUMO coupling tool TUDflow3D near-field and D3D far-field for WID	15
2.4	Implementation rheology in TUDflow3D for WID density currents	17
2.4.1	Introduction	17
2.4.2	Rheological model	17
2.4.3	Rheological characterization mud Calandkanaal	19
2.4.4	3D CFD simulation WID density current compared with lab experiment	21
2.4.5	Influence rheology on WID fluid mud layer flow	23
2.4.6	Conclusion	24
2.5	Quick scan analysis of influence SLR on sedimentation PoR	25
3	WP2: Large scale STM and WID experiments	28
3.1	Sailing Through Mud experiments	28
3.1.1	Summary	28
3.1.2	Methods	29
3.1.2.1	Characterization of fluid mud in the PL	29
3.1.2.2	Towing experiment in the WSF	30
3.1.3	Key findings	31
3.1.3.1	Objective 1: To find the link between sediment properties (density and salinity) and rheological properties.	31
3.1.3.2	Objective 2: To find how thixotropy of fluid mud can be quantified considering the non-Newtonian rheological modelling.	32
3.1.3.3	Objective 3: To relate existing analytical formulas for non-Newtonian fluids and how they can be used for estimating the plate resistance measured in the flume experiments.	32
3.2	Water Injection Dredging experiments	33
3.2.1	Summary	33
3.2.2	Methods	34
3.2.3	Key findings	35

3.2.3.1	Objective 1: To measure and analyse flow and sediment properties during the experiments in the watersoil flume for different parameter settings of water injection dredging.	35
3.2.3.2	Objective 2: To find the optimal parameter setting of water injection dredging to maximize production.	36
3.3	Recommendations on future experiments	37
3.3.1	Recommendation related to STM	37
3.3.2	Recommendation related to WID	37
3.3.3	Recommendation related to logistics	38
4	WP3: Data science for optimizing dredging	40
5	Overview detail reports and datasets TKI Prisma2	42
	References	43

List of abbreviations

Some often-used abbreviations in this document are defined below.

CFD	Computational Fluid Dynamics
COSUMO	Coupled Subgrid Models
D3D	Delft3D, which is a 3D hydrodynamic and sediment transport model in this case of the Port of Rotterdam area
NGD	Nautical Guaranteed Depth
PoR	Port of Rotterdam
PRISMA	PRogramma Innovatief Sediment MAnagement
SLR	Sea Level Rise
STM	Sailing Through Mud
TUDflow3D	3D CFD model for turbulent flow including sediment
WID	Water Injection Dredging

1 Introduction

1.1 Background

1.1.1 Introduction

The navigation in ports and waterways has to be safeguarded by maintenance dredging, removing sediments deposited by tide, river flows and currents. The volumes of dredged material have been substantially increased over the last 5 years (see Figure 1.1). As maintenance dredging and relocation of these deposits can be highly expensive, port authorities seek for tailor-made solutions to reduce the costs and at the same time guarantee safe navigation in ports and waterways.

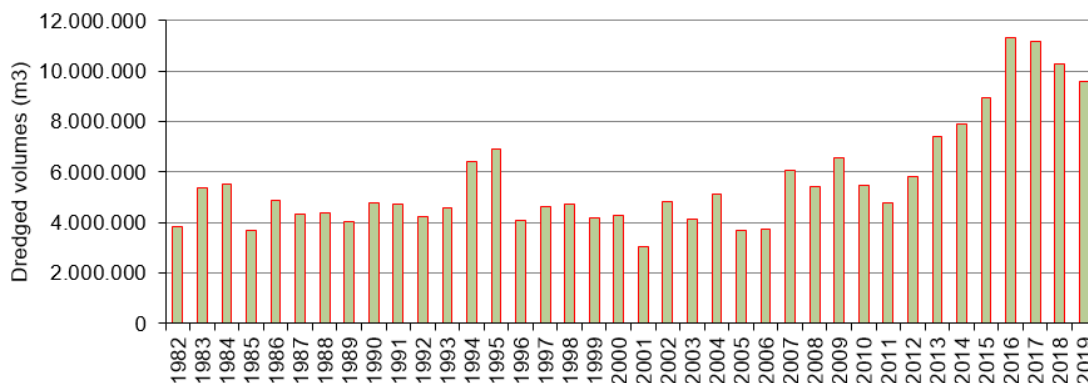


Figure 1.1. Dredged sediment volumes at the Port of Rotterdam from 1987 till 2019, excluding dredging by RWS in the access channels.

In order to keep ports and waterways accessible, more than 11 million m³ of sediment were dredged in 2017 (twice more than the volumes dredged in 2011). In 2017, about 77% of deposited sediment was mainly dredged by hopper dredgers at Maasvlakte, Europoort and Botlek areas (see Figure 1.2). The dredged sediment in these areas consist mainly of fine cohesive minerals forming silt layers.

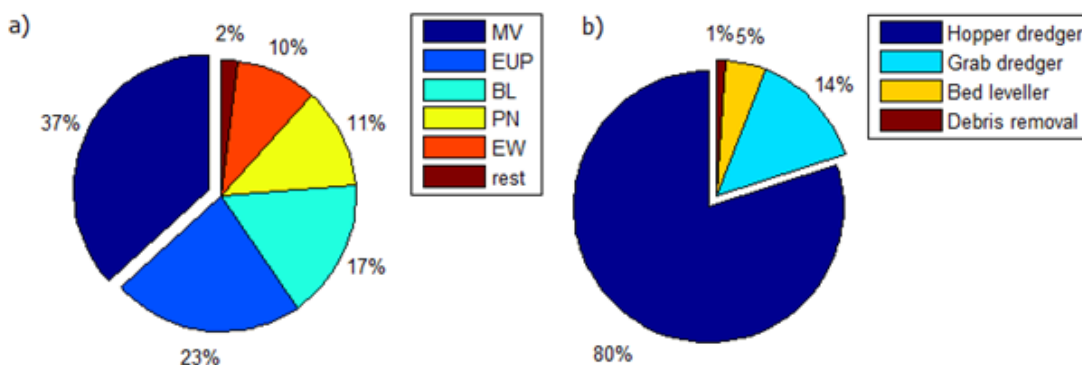


Figure 1.2. a) Dredged volumes at the port areas (MV: Maasvlakte, EUP: Europoort, BL: Botlek, PN: Pernis, EW: Eem-Waalhaven in 2017. b) Dredging methods by means of costs in 2017. From Kirichek et al., 2018a.

To minimize maintenance dredging costs and emissions several approaches exist. One could for instance optimize the dredging methodology. On the other hand, a potential improvement

could be to lengthen the interval of dredging in a smart way without reducing port functionalities. Water Injection Dredging (WID) is an example of the first and adjusting the dredging intervention protocol to a nautical depth based on rheological properties is an example of the latter.

1.1.2 Water injection dredging

For maintenance dredging of fine cohesive sediments Water Injection Dredging (WID) can be an efficient method, potentially more efficient as hopper dredging. WID entails the fluidization of sediment deposits by water jets (see Figure 1.3) injecting large volumes of water under low-pressure water jet nozzles. The injected water loosens the structure of the bed and the water-sediment mixture forms a fluid mud layer right above the bed. Field studies show that when a WID is operated with proper settings this dense fluid mud layer hardly mixes upwards and therefore transport of the mud layer remains close to the bed (Kirichek et al., 2020). The near-bed fluidized sediment deposit generates a gravity-driven density current up to 2 metres high (PIANC, 2013; Kirichek and Rutgers, 2020), transporting the sediment in a horizontal direction as a result of the density difference. Different transport distances from a few hundred meters to a few kilometres are reported in literature under favourable conditions. In the PoR area with limited bathymetric gradients and low tidal currents in the port basins, the transport distances are lower, in the order of a few hundred meters.

To avoid additional siltation in the vicinity and/or strong return flows, this option should be applied in combination with a favourable bed slope, ebb currents and/or a sediment trap from which sediment can be dredged more efficiently (Kirichek et al., 2020). The main beneficial application of a WID is foreseen for locations (e.g. at berths), which are not easily accessible by hopper dredgers. At short term the benefits may be large, but care should be taken that this is not counteracted by long term costs in the form of increasing dredging volumes.

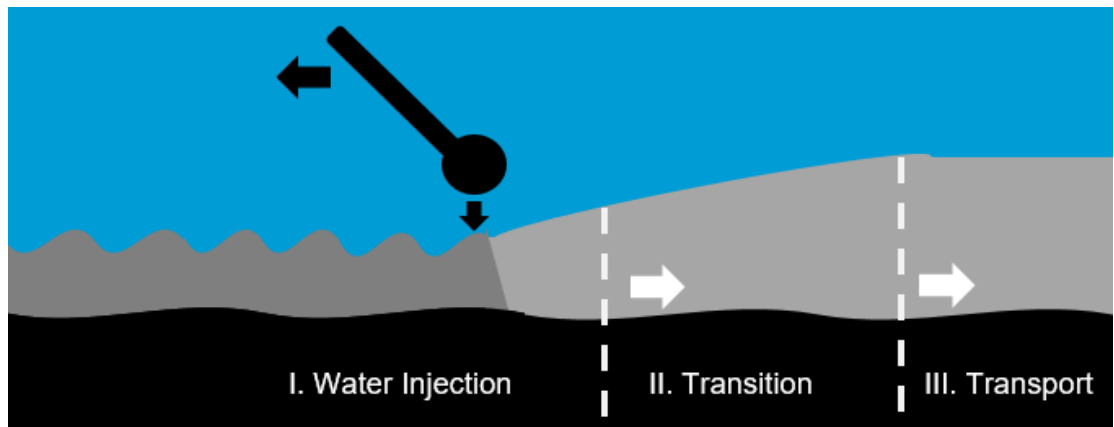


Figure 1.3 Phases of WID: I. Water injection and fluidization; II. Transition zone, where a density flow is created; III. Transport of the density flow. Adapted from Verhagen (2000)

1.1.3 Nautical bottom based on rheological properties

Another manner of reducing maintenance dredging efforts is by adjusting the moment when maintenance dredging is carried out without compromising port functions such as accessibility, navigability and safety. A conventional way to estimate the navigability in ports and waterways with fluid mud layers is done through the estimation of the nautical depth. This criterion ensures that vessels can safely navigate through areas where thick layers of fluid mud are detected. For practical reasons, the nautical depth is defined as a critical density (1.2 t/m^3 at PoR). The current nautical depth concept applied at PoR is shown in Figure 1.4.

It has long been recognized that a practical definition of nautical bottom should not only be based on density, but should also include the so-called rheological properties of the water-sediment mixture (Wurpts and Torn, 2005). Rheological properties (i.e. yield stress) provide a reliable criterion for nautical depth definition since they are related to the stress and shear history of the mud (Kirichek, 2016). Currently, the yield stress serves as a critical parameter for nautical depth in the Port of Emden (PIANC, 2014).

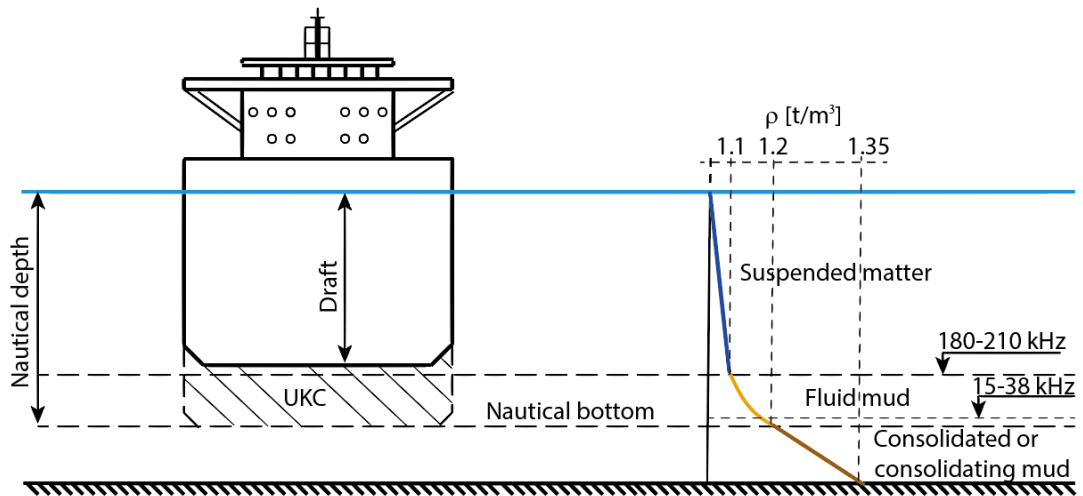


Figure 1.4 The nautical bottom concept at the Port of Rotterdam for the density limit of 1.2 t/m³. See Figure 1.5 for examples of fluid mud and consolidated mud.



Figure 1.5 Left: stiff consolidated mud. Right: weak fluid mud (from Kirichek et. al., 2018).

1.2 Objectives

Port authorities are striving to make port maintenance more efficient and sustainable. Within TKI project DEL 126 PRISMA II research is carried out for this purpose. PRISMA stands for PRogramma Innovatief Sediment Management". The overall aim of PRISMA is to reduce maintenance dredging costs and GHG (greenhouse gas) emissions. The TKI PRISMA II consortium consists of Port of Rotterdam, Rijkswaterstaat, dredging company Van der Kamp, Port of Hamburg, TU Delft, Deltares.

PRISMA II builds on the knowledge developed in previous projects. In a previous TKI Delta technology project (DEL048), the return flow of dredged sediment from the sea to the port mouth was examined (Hendriks and Schuurman 2017). This project is followed by another TKI Deltatechnology projects 'Modelling lokale slibdynamiek en aanslibbing Maasmond (MoMa)' (DEL089) (Cronin et al. 2019), that concerns the local sediment transport and sedimentation in

the port itself. The Deltatechnology TKI project 'Innovatief Sediment Management voor Havens (PRISMA)' (DEL 101) (Kirichek et al. 2021a) integrates the developed knowledge and brings new aspects, such as system knowledge, more in-depth modelling of fluid mud dynamics, innovative in-situ monitoring methods, water injection dredging and sediment trapping. Large scale far-field sediment transport simulation models of the entire port area have been developed as well as more detailed local near-field WID sediment transport simulation models (Kirichek et al. 2021b).

PRISMA II is focused on advancing the previously developed knowledge, model validation for a wider range of field conditions and on data from flume experiments carried out in a laboratory under controlled conditions, and on developing a quick assessment data-driven tool for optimizing dredging strategies. It consists of the following work packages:

1. Water Injection Dredging (WID) monitoring and modelling
2. Large scale experiments in water-soil flume Deltares
3. Data science for optimizing dredging

WP1 Water Injection Dredging (WID) monitoring and modelling

This work package consists of a monitoring campaign of WID actions in the Port of Rotterdam and of developing a rheological model implemented into 3D CFD (computational fluid dynamics) open-source software TUDflow3D in order to simulate the non-Newtonian fluid mud flow generated by WID. Within this work package a coupling tool is developed between the far-field Delft3D sediment model which captures the entire port area and a local near-field 3D CFD TUDflow3D model of WID actions. Sedimentation simulations are carried out for different periods and conditions with and without sea-level-rise with the far-field Delft3D model to increase our system knowledge and investigate the potential impact of sea-level-rise on sedimentation in the port area.

WP2 Large scale experiments in water-soil flume Deltares

In work package 2 two large scale experiments are designed and executed in the 33 m long, 2.4 m wide and 2.5 m deep water-soil flume of Deltares: a sailing through mud (STM) experiment and a water injection dredging (WID) experiment. Both experiments are conducted with mud from the Port of Rotterdam. Purpose of the experiments is to enhance our insights in the physical processes playing a role in STM and WID and to develop and validate numerical CFD models to be able to simulate those situations.

WP3 Data science for optimizing dredging

In the third work package data science is used to analyse the different available data streams of TSHD hopper dredging activities in the Port of Rotterdam. The aim is to optimize the dredging operations to be able to carry out maintenance dredging in the most efficient way with lower costs and GHG emissions.

1.3 Outline

In this overview report the different components of the TKI Prisma 2 project are summarized. More details can be found in the underlying reports. The purpose of this overview report is to get an overview of the results of the TKI Prisma 2 project and to have a clear document in which all components and underlying reports are summarised. This report continues with a description of the three work packages in the next three chapters. The report ends with an overview of the different reports and datasets generated in TKI Prisma 2.

2 WP1: Water Injection Dredging monitoring and modelling

2.1 Introduction

In WP1 the following tasks have been carried out:

- Analysis of field monitoring of WID in Calandkanaal area
- Development of COSUMO coupling tool between TUDflow3D near-field and D3D far-field models for WID density currents
- Implementation of rheology in TUDflow3D for WID density currents
- Improve system knowledge: Quick scan analysis of influence SLR on sedimentation PoR

2.2 Field monitoring WID Calandkanaal area

Water Injection Dredging (WID) is a dredging method that can be efficiently applied for fluidizing the bed by “injecting” water under pressure. Fluidizing the sediment by water injection, homogeneous fluid mud layers of a substantial thickness (up to 2 m) can be created (Kirichek and Rutgers, 2020). WID is particularly useful in areas that are not easily accessible by hopper dredgers and can be used to maintain an area at the required nautical depth. The fluid mud layers generated through WID have a weak shear strength and are ideally transported as a density current away from the dredged area.

The application of WID could cause negative environmental effects. The fluid mud layer generated by WID might be vertically mixed through the water column if mixing is sufficiently strong. Therefore, turbidity levels near the surface could increase and reduce the capacity of light to penetrate the water column. Reduced visibility can influence aquatic life negatively.

Turbidity measurements in an area where WID is performed are analyzed to determine to which extent WID influenced the observed turbidity and SSC throughout the water column at several sites located in vicinity of WID areas, during and after WID was applied. The gained insight should provide input to determine the potential environmental impact of the WID activities.

The PoR performed WID a couple of days including the 22th of February of 2021 at the Calandkanaal and Nijlhaven. To assess the environmental impact, measurements during and after the WID have been conducted. Thus, the first survey was performed on the same day of the WID activities (22th) and the second survey was performed after WID at the 25th. All measurements have been performed over at the same transects, see Figure 2.1:

- A. Nijlhaven (N)
- B. Breddiep (BD)
- C. Beerkanaal (BK)
- D. Calandkanaal (CK)

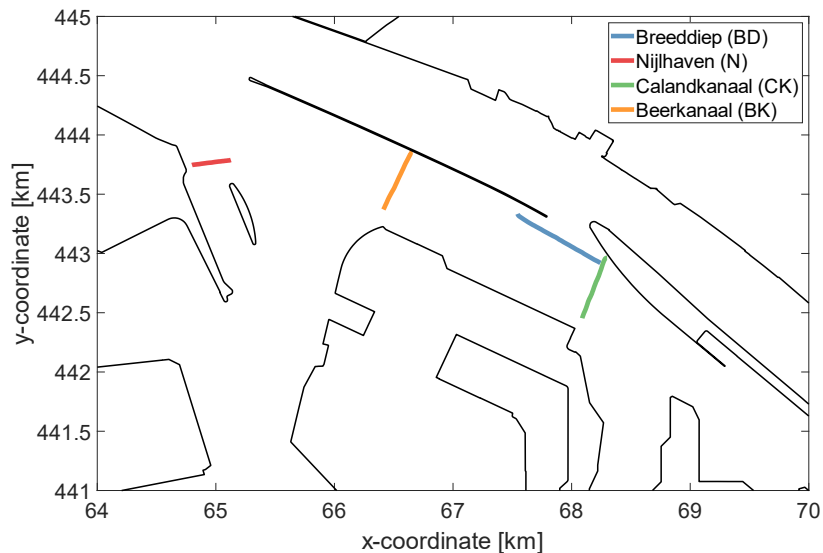


Figure 2.1 Overview of the four transects. The shown transects are the actual ADCP tracks of 22th of February.

At all transects, vertical turbidity profiles were taken using the OBS mounted to the Surveyor 2. During the 22th 17 profiles were measured and during the 25th 13 profiles. The average profiles are visualized in Figure 2.2. For all transect the following holds: near the bed the observed turbidity is significantly higher after WID compared to the turbidity during WID and near the surface the observed differences are marginal (maximal 2.5 FTU). This is especially visible for the location CK, BD and N. Here a significant increase in the turbidity is observed approximately between 17.5 m and deeper. BK shows a distinctive profile with a mid-column increase from 10 to 20 FTU and no substantial increase near the bed. In conclusion, Figure 2.2 indicates that at CK, BD and N a layer with a relative high turbidity has developed near the bottom after WID. During both surveys the influence of WID on the turbidity is hardly visible at mid column and above.

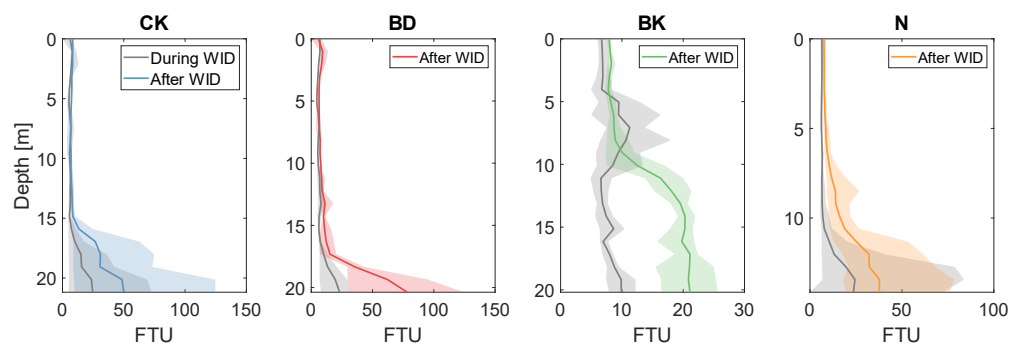


Figure 2.2 Average turbidity profile (FTU) during and after WID shown for each location. The coloured contours show the minimum and maximum observed values spread.

The complete analysis of the monitoring campaign can be found in a separate memo (Keulen, 2021). A summary of the main findings of the analysis of this monitoring campaign is given below:

- The directly measured turbidity profiles, from the OBS, show that the surface and mid-column turbidity was low and comparable during and after WID. Higher near-bed turbidity values were observed in some of the profiles during WID and in most profiles taken after WID. This indicates that the influence of WID on turbidity seems to be

limited to the near-bed region, both during WID and in the settling and consolidation phase afterwards.

- Between day 1 and 2 of the monitoring campaign the hydrodynamic conditions were different for some transects. At the Beerkanaal, the flow had an opposite direction during and after WID. This makes direct comparisons between the turbidity profiles less straightforward without normalizing for the hydrodynamic conditions.
- Finally, water samples collected during the measurement campaign show relatively low sediment concentrations. Typical near surface SSC of ~5 mg/l and near bed SSC's of between 10-50 mg/l are observed during and after WID. This again indicates the SSC near the water surface was not significantly increased by WID.

This brief two-day monitoring campaign in the Calandkanaal-Beerkanaal area, conducted during and after WID, indicates that WID increases turbidity in the lower parts of the water column near the bed. The difference in turbidity near the surface during and after WID was insignificant compared to the increase in the lower parts of the water column. A caveat is that it is not fully certain that the complete plume has been captured in the measurement profiles.

2.3 COSUMO coupling tool TUDflow3D near-field and D3D far-field for WID

The dispersion of sediment due to Water Injection Dredging depends on the detailed behaviour (mixing, spreading, etc.) in the near-field zone as well as the subsequent transport driven by the ambient hydrodynamics in the far-field zone. The near-field sediment plume behaviour can be modelled in detail by means of CFD solvers like TUDFlow3d. These CFD solvers, however, are typically computationally too heavy to model the large scale far-field behaviour. For the far-field behaviour software packages like Delft3D could be used.

A model coupling is developed between TUDFlow3d near-field results and a Delft3D4 far-field model. This model coupling is based on an in-house available coupling interface (COSUMO). COSUMO (Coupled Subgrid Models) is a generic interface that was set up to dynamically couple Delft3D to other software packages for integral time-efficient modelling assessments. Every coupling interval, Delft3D writes a communication file, which is automatically picked up by the MATLAB-based program COSUMO. COSUMO prepares the required input for the near-field model. The output of the near-field model is subsequently processed by COSUMO into the format required for Delft3D. COSUMO has been successfully applied in multiple projects for power and desalination plants. In these projects, COSUMO facilitated the communication between plume models, like CORMIX, that compute the detailed mixing characteristics near the point of discharge and Delft3D, which models the larger scale plume dispersion. COSUMO was also used to couple the salt intrusion due to sluice operations at the Panama Locks and the IJmuiden Locks (computed by WANDA-Locks) to the inland Delft3D models.

For the development of COSUMO coupling of WID density currents the following approach is chosen. Given the computationally heavy near-field TUDflow3d computations, it was decided to run a set of near-field computation prior to the far-field computations, see Figure 2.3. A fully dynamic two-way coupling for this application would require too much time. The sediment plume behaviour in the near-field computations was analysed and characterized in a database. During the far-field Delft3D computation, COSUMO will select the best-fitting near-field computation from the database and prescribe the associated plume behaviour to the Delft3D model.

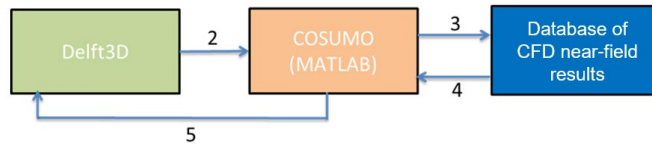


Figure 2.3 COSUMO coupling CFD near-field to Delft3D far-field

An example of the coupled WID density current is given in Figure 2.4. The coupling is performed on the cyan dashed circle. Some details of the resulting sediment concentration are different mainly because of differences in grid detail. The near-field CFD grid is much finer than the far-field Delft3D grid and therefore some local details of the near-field results can never be captured in the far-field coupled simulation. This is inevitable because of the different purpose, extent and grid resolution of a near-field model compared to a far-field model. In general, the overall picture is very comparable.

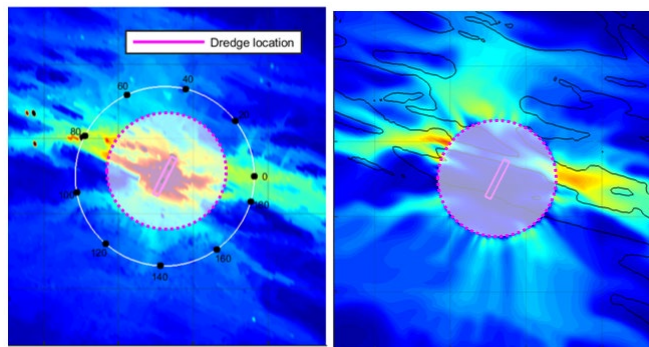


Figure 2.4 Example in the direct vicinity of the WID of the simulated near-field TUDflow3D sediment concentration of a WID (left) and the simulated far-field Delft3D sediment concentration of a WID after coupling via COSUMO (right). The coupling is performed on the cyan dashed circle.

A comparison of the resulting WID density current from the original TUDflow3D CFD near-field simulation and the coupled far-field Delft3D simulation is given in Figure 2.5. The WID is moving from west to east along a 300m working trajectory six times. In between, while moving back to the starting location, it is non-productive. The sediment concentration image during the fifth passage as shown in Figure 2.5 is quite comparable even though the grid resolution in the Delft3D far-field simulation is 5x coarser. The near-field characterization of the WID density current as simulated by the CFD model can be captured accurately in the far-field Delft3D simulation by the locally adjusted source terms for Delft3D determined with COSUMO.

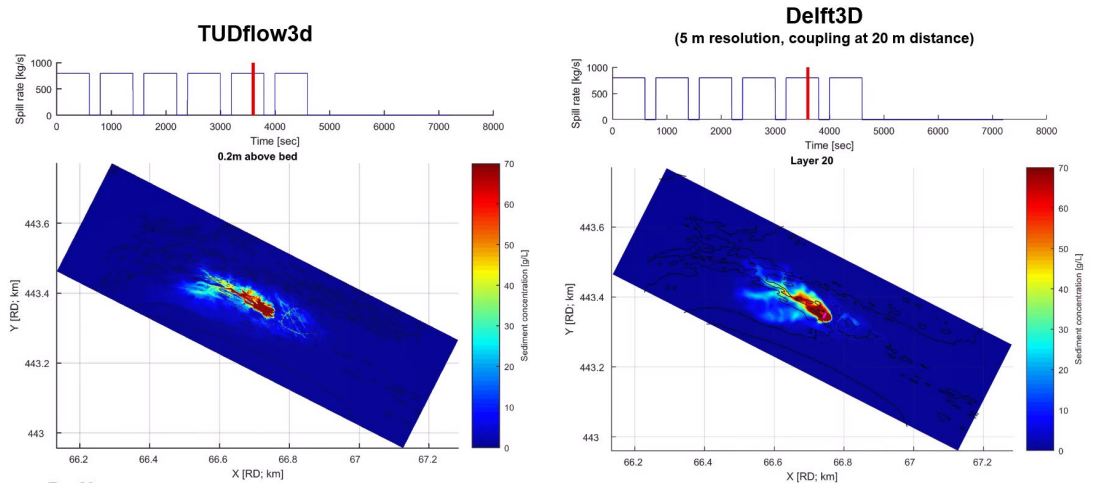


Figure 2.5 Example of the resulting WID plume of the simulated near-field TUDflow3D sediment concentration of a WID (left) and the simulated far-field Delft3D sediment concentration of a WID after coupling via COSUMO (right).

More details about the COSUMO coupling tool for WID density currents can be found in Verbruggen (2022).

2.4 Implementation rheology in TUDflow3D for WID density currents

2.4.1 Introduction

A rheological model was implemented in the CFD model to capture the non-Newtonian behaviour of a fluid mud layer generated by WID. This has been the graduation work of E. ten Brummelhuis (Brummelhuis 2021) and has been presented at the world dredging conference in Copenhagen in 2022: (de Wit, Brummelhuis, Talmon 2022).

2.4.2 Rheological model

The rheology of a non-Newtonian fluid, like fluid mud, is modelled by the Bingham model. For the modelling of non-Newtonian fluids different constitutive equations exist, among which the Bingham model is most popular due to its simplicity. Fluids that obey this model are known as visco-plastic fluids and characterised by the existence of a yield stress τ_B that must be exceeded before it will deform or flow. Once the yield stress is exceeded by the applied stress, the flow curve grows linearly by a proportionality constant μ_B also known as the Bingham plastic viscosity. In full tensorial form the Bingham model reads (Beverly & Tanner, 1989):

$$\begin{aligned} T_{ij} &= 2 \left(\mu_B + \frac{\tau_B}{|\dot{\gamma}|} \right) S_{ij} & \Leftrightarrow & |\tau| > \tau_B, \\ S_{ij} &= 0 & \Leftrightarrow & |\tau| \leq \tau_B, \end{aligned} \quad (5)$$

where T_{ij} is the stress tensor, S_{ij} the strain rate tensor and $|\tau|$, $|\dot{\gamma}|$ are the generalised shear stress and shear rate respectively, given by (Derksen & Prashant, 2009):

$$\begin{aligned} |\dot{\gamma}| &= \sqrt{2\Pi_{\dot{\gamma}}} = \left[2 \sum_{i,j=1}^3 S_{ij} S_{ij} \right]^{1/2}, \\ |\tau| &= \sqrt{\frac{1}{2}\Pi_{\tau}} = \left[\frac{1}{2} \sum_{i,j=1}^3 \tau_{ij} \tau_{ij} \right]^{1/2}. \end{aligned} \quad (6)$$

To account for the discontinuity as the shear rate approaches zero, the Papanastasiou viscosity regularisation method is applied. This method adds an exponential term to the Bingham model to smooth the stress discontinuity ensuring a finite viscosity at low shear rates. In tensorial form the Bingham-Papanastasiou equation becomes equal to (Papanastasiou & Boudouvis, 1997):

$$\begin{aligned} T_{ij} &= 2 \left(\mu_B + \frac{\tau_B}{|\dot{\gamma}|} [1 - e^{-m|\dot{\gamma}|}] \right) S_{ij} & \Leftrightarrow & \quad |\tau| > \tau_B, \\ S_{ij} &= 0 & \Leftrightarrow & \quad |\tau| \leq \tau_B, \end{aligned} \quad (7)$$

with m the viscosity regularisation parameter. The non-Newtonian constitutive equation is adopted in the Navier-Stokes equations by a so-called apparent viscosity η , which is added to the eddy viscosity used in the momentum equations. In the diffusivity, used in the sediment transport equations, the apparent viscosity is not included. The total viscosity used in the momentum equations thus consists of the sum of the molecular viscosity, turbulent eddy viscosity and apparent viscosity to account for rheology. In zones where rheology is important the apparent viscosity is much larger than the turbulent eddy viscosity and the viscous flow behaviour is governed by the apparent viscosity leading to laminar flow. In zones without non-Newtonian fluid only the molecular and turbulent viscosity remains leading to turbulent flow. In principle this framework should be able to handle the laminar-turbulent transition, but this has not been studied in detail. Especially because the Large Eddy Simulation approach (giving resolved turbulent eddies on the grid) is used to capture turbulence instead of a Reynolds averaged approach like K-Epsilon the laminar-turbulent transition from non-Newtonian to Newtonian flow is very pronounced in different flow character in the model. The apparent viscosity is given by:

$$\eta = \mu_B + \frac{\tau_B}{|\dot{\gamma}|} [1 - e^{-m|\dot{\gamma}|}]. \quad (8)$$

The numerical implementation of the Bingham-Papanastasiou model was verified against two benchmarks from known literature. This consists of an analytical steady-state solution of the plane Poiseuille flow (Goeree, 2018) and results of the classical lid-driven cavity problem by Syrakos et al. 2014.

To relate the Bingham model parameters to a soil property, like volumetric concentration of fine-grained solids, two models were used, namely:

1. Thomas
2. Jacobs and van Kesteren

These models have been successfully applied in the modelling of oil sand tailings (Talmon et al. 2016) and can be adapted for fluid mud density currents with an appropriate parameter study.

Based on an experimental study on the influence of coarse granular particles in mine tailings, Thomas (1999) modified the well-known expression by Krieger & Dougherty, (1959) resulting in the following relationships for yield stress and viscosity:

$$\tau_B = C_y \left(\frac{\phi_{fi}}{\phi_w + \phi_{fi}} \right)^p \left[1 - \frac{\phi_{sa}}{k_y \phi_{sa_{max}}} \right]^{-2.5}, \quad (9)$$

$$\mu_B = \mu_w \exp \left(C_\mu \frac{\phi_{fi}}{\phi_w} \right) \left[1 - \frac{\phi_{sa}}{k_\mu \phi_{sa_{max}}} \right]^{-2.5}, \quad (10)$$

Where ϕ_{fi} , ϕ_{sa} and ϕ_w are the volumetric concentrations of fines, sand and water respectively, additionally $\phi_{sa_{max}}$ is the concentration at maximum packing density. C_y , C_μ , p , k_y and k_μ are empirical correlation parameters. The non-Newtonian behaviour, caused by the fines, is incorporated into the first part of the relationships, and the second part contributes to the influence of coarse granular particles.

The fundamental idea of the second model by Jacobs and van Kesteren is that the relative water content WC_{rel} can be used as governing parameter for the baseline rheological behaviour. The relative water content is defined as the water content WC normalized by the plasticity index PI :

$$WC_{rel} = \frac{WC}{PI} \approx \frac{\rho_a \phi_w}{A_{cl} \rho_s \phi_{cl}} \quad (11)$$

Where ϕ_{cl} is the volumetric concentration of clay and A_{cl} is the colloidal activity of clay (Skempton, 1953). Implementation of the relative water content into a rheological model leads to the following relationships:

$$\tau_B = K_y \left(\frac{WC}{PI} \right)^{B_y} \exp(\beta\lambda), \quad (12)$$

$$\mu_B = \left[\mu_w + K_\mu \left(\frac{WC}{PI} \right)^{B_\mu} \right] \exp(\beta\lambda), \quad (13)$$

Where K_y , K_μ , B_y , B_μ are empirical parameters depending of the type of clay. The exponential term accounts for the internal friction induced by coarse granular particles, also known as the solids effect (Bagnold, 1956).

2.4.3 Rheological characterization mud Calandkanaal

The empirical parameters of the rheological models have been determined using an extensive rheology study on fluid mud from the Calandkanaal, Port of Rotterdam in the Netherlands. A large sample of mud taken from the lab WID experiment is analysed using a rotational rheometer. The initial sample is diluted by both fresh- and seawater several times creating eight subsamples. The dilution ratios of the subsamples range from 1.00:0.00, no additional water added, to 1.00:2.00, which entails one unit mass of mud and two unit masses of water which gives a total of three unit masses of mixture.

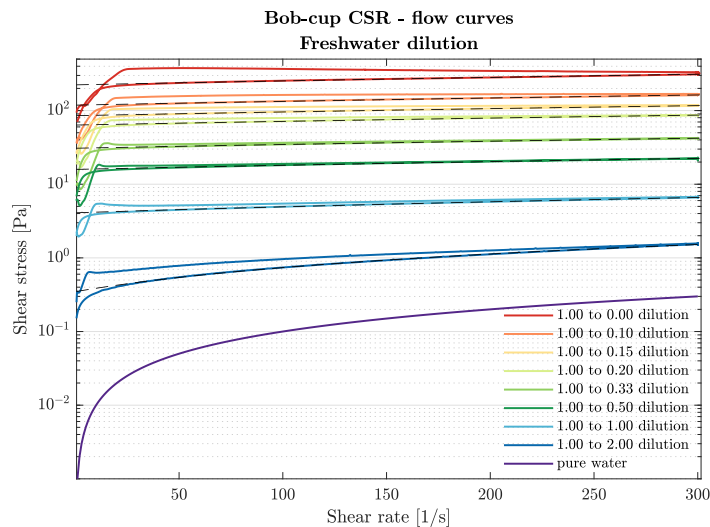


Figure 2.6 Example of rotational rheometer flow curves for different dilutions of mud from Calandkanaal Port of Rotterdam and fitted Bingham yield stress and viscosity for each dilution indicated in black dashed lines

Flow curves of each sample were created by the rotational rheometer in a controlled shear rate (CSR) operational mode utilizing the bob-cup measuring geometry. The Bingham model parameters can be deduced by fitting the Bingham model to the down-ramp of the flow curves, see Figure 2.6. The Bingham fits in the graph reveal a difference at low shear rates. This disappeared when we applied a vane for measuring element, similar to reported in Talmon et al. (2021) for fluid mud from the Beerkanaal in Port of Rotterdam.

Both rheological models account in some way for the solids effect, which is the internal friction induced by coarse granular particles, due to the presence of coarse granular material like sand. However, it is assumed that this effect is negligible in fluid mud density currents because mud from the Port of Rotterdam contains little to no sand particles. This assumption is supported by multiple particle size distributions (PSD's), measured by a static light scattering technique, taken from port samples (Kirichek et al., 2021). According to these PSD's the vast majority of particles fall within the silt size class (between 2 and 63µm), and for this reason the solids effect is disregarded in the parameter study. The empirical parameters are estimated by curve fitting the models to the measured Bingham yield stress and viscosity for different dilutions of the mud, see Figure 2.7. The results of the curve fits of both models are very close to each other and correspond very well with the measurements. Table 2-1 summarizes the empirical model parameters for both fresh- and seawater dilutions.

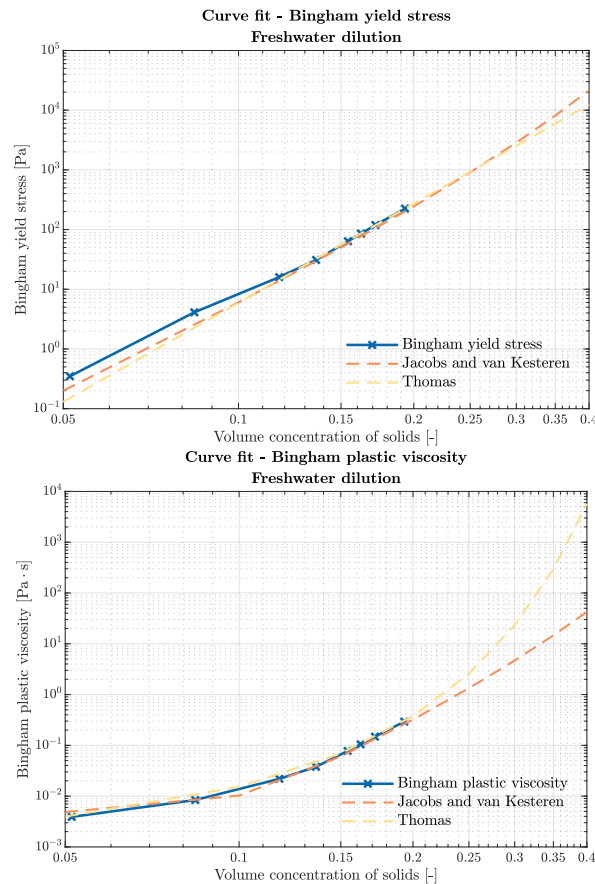


Figure 2.7 Example of measured and fitted Bingham yield stress [left] and Bingham plastic viscosity [right] for different volume concentrations of mud from Calandkanaal Port of Rotterdam

Table 2-1 Obtained model constants for the Jacobs and van Kesteren and Thomas rheological models for mud from Calandkanaal Port of Rotterdam

Jacobs and van Kesteren		
Parameter	Freshwater	Seawater
A_{cl}	1.0	1.0
μ_w	0.0047	0.0044
K_y	1.7868e+3	1.3919e+3
B_y	-4.5655	-4.2698
K_μ	2.8018	2.1599
B_μ	-4.9944	-4.7014

Thomas		
Parameter	Freshwater	Seawater
μ_w	0.0012	0.0015
C_y	1.9390e+6	9.8974e+5
p	5.5154	5.1748
C_μ	23.1036	21.4058

2.4.4

3D CFD simulation WID density current compared with lab experiment

CFD WID density current simulations of large scale WID experiments in the 33m long, 2.4 m wide and 2.5m deep water soil flume of Deltares are presented in this section. These WID experiments are prescribed in more detail in Section 3.2. Two runs (run A and B) from the first set of experiments are used for CFD comparison, see Table 2-2. The input of these simulations is defined differently from the WID simulations presented in (Brummelhuis 2021) because in those simulations an inconsistency was found. The input and results presented in this section come from (de Wit, Brummelhuis, Talmon 2022). The measured initial bed level, measured bed level after the WID has fluidized the top layer and ramp height in the experiment are used as input in the CFD simulations together with the WID jet-bar volume flux Q per unit width [$m^3/s/m$] and sediment source flux S per unit width [$kg/s/m$]. To promote generation of 3D flow features in the CFD model the WID source fluxes are not injected over the complete width, but over three separate zones. Due to uncertainty in the exact source flux of sediment in the experiment simulations with the source flux corresponding to the measured penetration are performed and simulations with 40% larger source flux which would correspond better with the observed density current fluxes for these experimental runs. The initial mud concentrations of the four runs in Table 2-2 ranges from 0.07 to 0.18 ($200-470 kg/m^3$) leading to initial yield strengths of $\sim 1 Pa$ to $\sim 100 Pa$.

Table 2-2 CFD input for experimental WID cases

Run name	Ramp height	Initial bed level	WID penetration	WID speed	WID production S per unit width	WID discharge Q per unit width
Exp 1 run A	0.5m	0.56m	0.1 m	0.25 m/s	11 kg/s/m	0.05625 $m^3/s/m$
Exp 1 run A S+40%	0.5m	0.56m	0.14 m	0.25 m/s	15 kg/s/m	0.05625 $m^3/s/m$
Exp 1 run B	0.4m	0.46m	0.17m	0.25 m/s	19 kg/s/m	0.05625 $m^3/s/m$
Exp 1 run B S+40%	0.4m	0.46m	0.24m	0.25 m/s	26 kg/s/m	0.05625 $m^3/s/m$

A 0.84m wide slice of the water soil flume is used as 3D CFD model domain, see Figure 2.8. To save computation time not the entire width of the water soil flume is included. This is allowed because the experimental set up is a 2DV width-averaged setup. The lateral boundaries in the CFD model are periodic boundaries. The boundary at $x=-27$ is a closed boundary and at $x=6m$ an outflow boundary is used. The top boundary is a free slip symmetry boundary and the bottom boundary at the mud bed consists of a partial slip law of the wall boundary with a Nikuradse bed roughness of 0.01 mm. The computational grid consists of 1 million cells with a resolution of $\Delta x = 0.06 m$, $\Delta y = 0.0525 m$ and $\Delta z = 0.02 m$. Near the ramp the grid is refined in x-direction to $\Delta x = 0.02 m$.

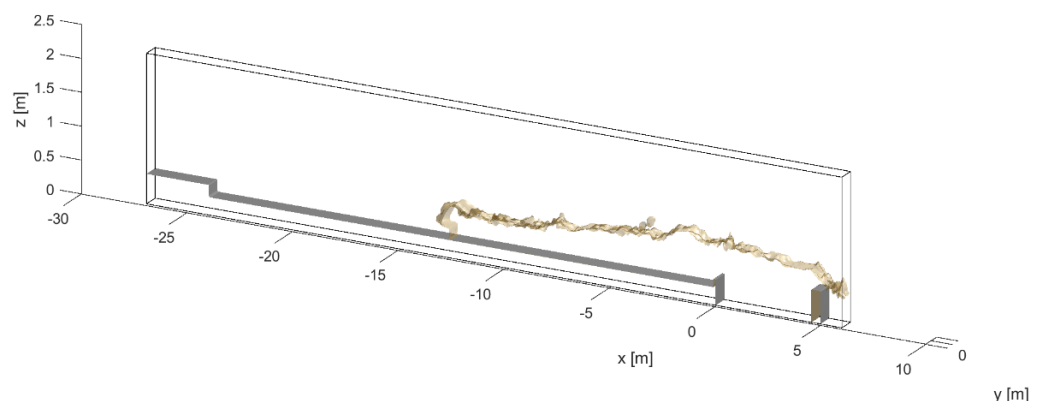


Figure 2.8 Image of computational domain for WID experiment A and B. The grey contour shows the mud bed at the end of the simulation and the crest at $x=0$ together with an obstacle near the outflow boundary which was present in the experiment. The brown concentration contour shows the WID density current after 50s when the WID jet-bar has moved with $0.25m/s$ to $x=-12.5m$.

Simulations are carried out with mud rheology included and without rheology (Newtonian). To include mud rheology the Jacobs and van Kesteren model parameters for fresh water dilution are used. A test with the Thomas fresh water parameters gave similar results. A Papanastasiou viscosity regularisation parameter $m=20$ has been used. Simulations are carried out with and without initial WID jet-bar momentum. In the experiment the WID jet-bar injects water from 35 mm nozzles at a speed of 5.8 m/s. As explained before, this level of detail cannot be captured on the CFD grid employed in this study, which focuses on simulating the resulting fluidized mud density current. However, a jet-integral model Jetplume (Lee and Chu 2003) has been used to determine the jet flux and jet momentum 10 cm from the nozzle exit when flowing in water. In some of the simulations this vertical momentum has been included in the WID jet-bar source in the CFD model and in other simulations this vertical momentum is neglected. In the end the following five simulations are compared for experiment 1 run A and experiment 1 run B:

- Rheology and initial vertical momentum (W_{ini})
- Rheology and neglecting vertical momentum
- Without rheology, but with initial vertical momentum (W_{ini})
- Without rheology and neglecting vertical momentum
- Rheology and initial vertical momentum and WID source S+40%

Natural Calandkanaal mud from a sample with concentration 1 kg/m^3 collected 1 m above the fluid mud layer consists of a wide range of microflocs to macroflocs with mud floc sizes of 10-400 μm and settling velocities of 0.04-20 mm/s (Kirichek et al. 2021). The Calandkanaal mud used in the experiment has been tested in a settling column test which gave an average settling velocity of 3.6 mm/s and a gelling concentration of 170 kg/m^3 beyond which settling stops. When conducting WID it can be expected that macroflocs will be destroyed by the high shear from the WID jets. Therefore, in the simulations mud is given a settling velocity of 1 mm/s and a gelling concentration in the hindered settling formulation of 170 kg/m^3 . This gelling concentration corresponds to a Bingham yield stress of about 1 Pa marking the transition from no influence of rheology to starting influence of rheology.

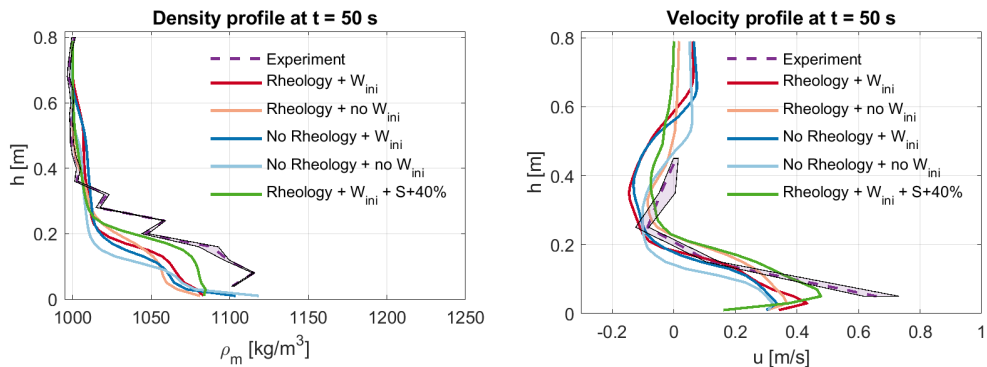


Figure 2.9 Comparison of measured and simulated density and velocity profiles at the crest at the end of the mud bed for experiment 1 run A

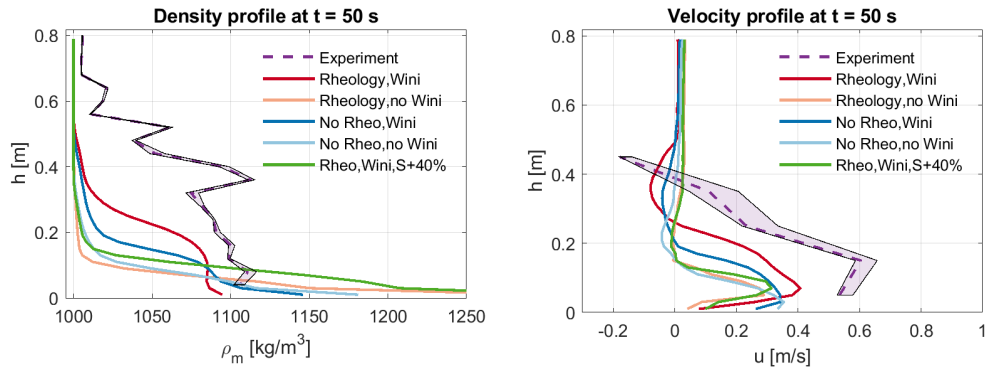


Figure 2.10 Comparison of measured and simulated density and velocity profiles at the crest at the end of the mud bed for experiment 1 run B.

The simulated vertical density profiles and velocity profiles above the crest of the ramp halfway the experiment after 50s are compared with the measured ones in Figure 2.9 and Figure 2.10. The density of $\sim 1100 \text{ kg/m}^3$ and velocity of $\sim 0.4 \text{ m/s}$ is in the same range as the scarcely available field scale WID density current measurements indicating velocities of $\sim 0.3\text{-}0.7 \text{ m/s}$ and densities of $\sim 1050\text{-}1100 \text{ kg/m}^3$ (PIANC 2013, Van Rijn). The density current height of $\sim 0.4\text{m}$ for this experimental set up is lower than the observed field scale heights of $\sim 0.5\text{-}3\text{m}$.

The simulated results for experiment 1 run A are better than for run B and in both cases inclusion of rheology improved the results. The shape of the velocity profile with positive velocities below and opposite entrainment flow above this layer is captured correctly in the CFD model. For run A the simulated density current height and velocity profiles are close to the experimental ones and for run B they deviate more. A potential explanation for this extra deviation between experiment and CFD model in run B is that run B is the second WID trail on the same bed of run A. It might be possible that in run A a top layer of mud has been diluted but did not flow away and now in run B on the same bed it is flowing away with extra dilution from the second WID trail. This is not included in the CFD model WID source term approach.

Especially given the difficulty that there is uncertainty in the exact WID sediment source flux of the experiment and it is very well possible that the mud bed with real Calandkanaal mud is not perfectly homogeneous, the results are a step to understand the non-Newtonian flow of a WID density current better.

2.4.5 Influence rheology on WID fluid mud layer flow

In Figure 2.11 and Figure 2.12 two simulated cases with/without rheology from experiment 1 run B are used to illustrate the potential impact of rheology on the WID fluid mud flow. For these examples the high yield stress in the high-density region on a WID fluid mud layer can laminarise the flow without rheology this behaviour is not included resulting in a very different flow pattern.

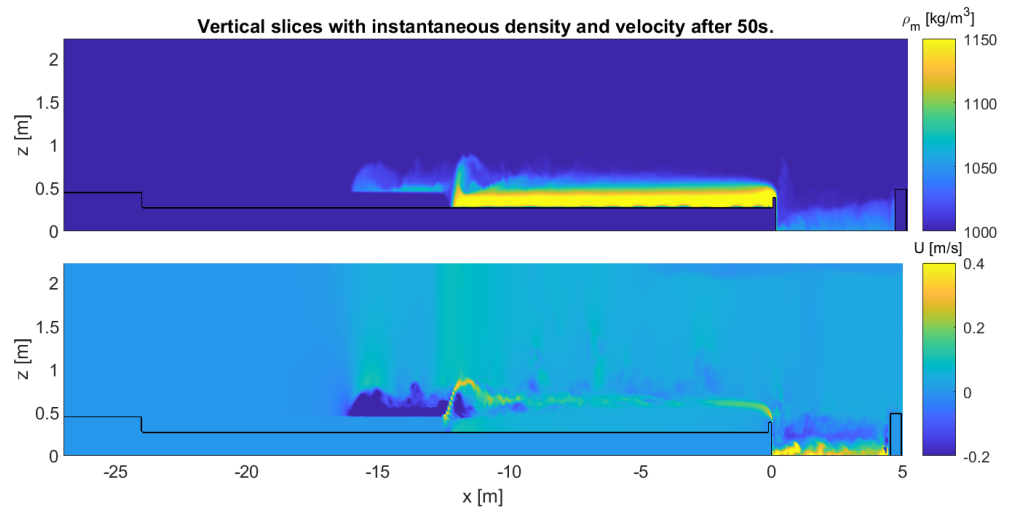


Figure 2.11 Instantaneous density and velocity at time=50s for CFD simulation of experiment 1 run B with rheology, no vertical momentum

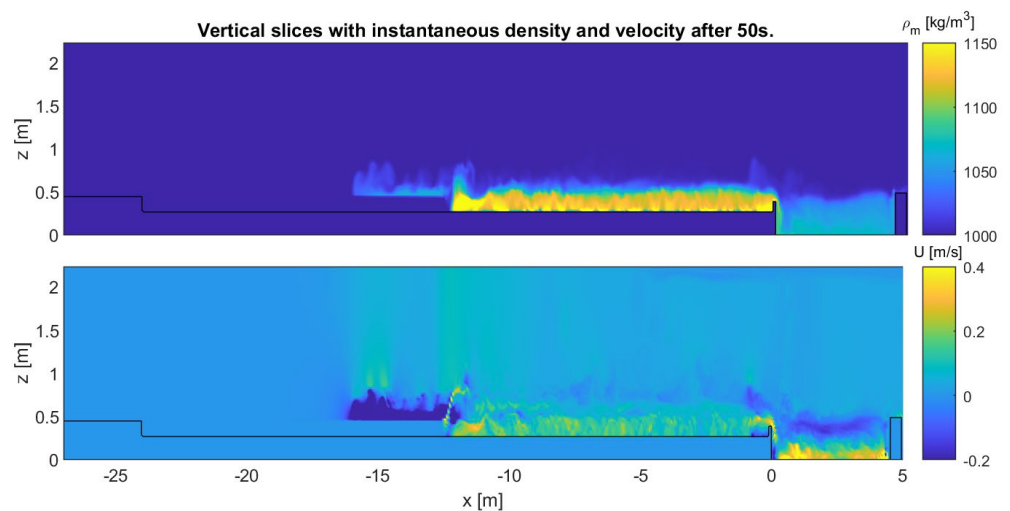


Figure 2.12 Instantaneous density and velocity at time=50s for CFD simulation of experiment 1 run B without rheology, no vertical momentum

2.4.6 Conclusion

A CFD model can tell us in what direction the fluidized mud layer from a WID is expected to move, how fast it will be moving, whether it will mix in the vertical and where it stops moving and will deposit. This behaviour is influenced by rheology and therefore it is important to include this in the calculations. Inclusion of rheology in CFD model TUDflow3D is now possible because of the graduation work of Brummelhuis (2021). It was found that the rheological behaviour of fluid mud from the Calandkanaal area can be described accurately by simple curve fits. Comparison of the CFD WID results with the experimental results proved that the CFD model gives realistic velocity and density profiles for the moving fluid mud layer from WID and inclusion of rheology improved the model results. There remain differences between the CFD results and the lab measurements which require further study in a follow up. With the inclusion of mud rheology in the CFD model the non-Newtonian flow of a WID density current can be understood better which is useful to optimize WID operations and assess potential environmental impact.

2.5 Quick scan analysis of influence SLR on sedimentation PoR

It is likely that climate change is going to impact sedimentation processes in harbours. Because of complex interactions between different driving processes such as wave-induced resuspension at sea, tidal transport and gravitational circulation it is unknown how strong this impact will be and if the impact is different for port basins close to the sea and more upstream. In this quick scan a first exploration on one aspect of climate change, namely the impact of sea level rise (SLR), on sedimentation is presented based on two approaches: 1) complex 3D sediment transport simulations of the port of Rotterdam and 2) a quick scan tool SEDHAR. The complex 3D model used in this study is the already existing OSR (Operationeel Stromingsmodel Rotterdam) Delft3D sediment transport model of the Port of Rotterdam (PoR), see Figure 2.13.



Figure 2.13 Domain of the OSR-NSC model, which was used as a basis in this model study (light blue).

Different scenarios are simulated comprising of different periods with different conditions. In the scenarios boundary conditions such as river discharge, tide and waves are varied. The base scenario consists of the conditions belonging to May 2016 for which the Delft3D sediment transport model was compared with dredging volumes. Purpose of the scenario simulations is twofold: 1) investigate the potential impacts of SLR on sedimentation and 2) investigate the robustness and validity of the Delft3D sediment transport model results of May 2016 for different periods and conditions.

The different periods are selected for their difference in river discharge. May 2016, the default period, has a medium river discharge ($Q_{Lobith} \sim 2500 \text{ m}^3/\text{s}$). The other two periods are June 2016 with a high river discharge ($Q_{Lobith} \sim 4000 \text{ m}^3/\text{s}$) and October 2016 with a low river discharge ($Q_{Lobith} \sim 1100 \text{ m}^3/\text{s}$). For the different periods not only the river discharges are different, but inevitably also other forcings such as wind and wave conditions are somewhat different, as the numerical model is forced with actual hydro-meteo conditions. To assess the influence of SLR, simulations with and without 1m SLR are compared. 1m SLR is applied in a schematised way by only adjusting the sea water level with 1m without changing the bathymetry and keeping all other conditions like the river discharge, sediment boundary conditions and the wind/wave conditions unchanged.

It is found that the sedimentation in sub-basins in the Port of Rotterdam area varies strongly (up to +49% and -77%) for the different periods investigated, but the total sedimentation in the entire port area differs less (+/- 22%). This shows that the overall sedimentation results

obtained with the Delft3D sediment transport model for the default period are not exceptional and can be used to give an indication of the expected year-round sedimentation.

The scenarios with SLR show that 1m SLR as simulated schematically impacts the hydrodynamics, the dynamics of the salt wedge, the influence of wave-induced resuspension on the North Sea and subsequently the sedimentation in the port area noticeably. Especially for port basins near the location of the estuarine turbidity maximum at the end of the intrusion of the salt wedge the sedimentation is altered by SLR. Sedimentation in the Botlek (-14%) and Europort (-22%) slightly decreases in the scenario with SLR, whereas sedimentation increases in the basins near the new location of the salt wedge (i.e. Pernis, Waalhaven, Fruithaven, approx.+15%).

SEDHAR is found to be a fast tool to get an indication of the sedimentation in sub-basins and change in sedimentation for different conditions such as SLR. SEDHAR is a semi-empirical rapid assessment tool (v. Rijn, 2005), which may be regarded as a 'light' version of Silthar (Eysink, 2004) that computes sedimentation in port basins. It uses three components of the sediment exchange between a basin and the adjacent water:

1. Tidal prism/exchange
2. Horizontal eddy/circulation driven in the along-basin mouth direction
3. Vertical exchange due to density differences/stratification

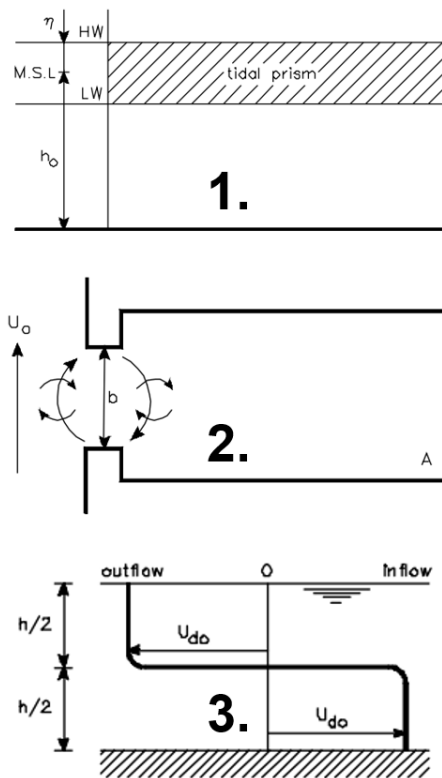


Figure 2.14 Three sediment transport components in SEDHAR

The SEDHAR results (see Figure 2-15) are summarized as follows:

- Deposition rates in the Waalhaven, Botlek, Amazonehaven port basins are predicted to be in the order of $450, 850$ and $250 \times 10^3 \text{ m}^3/\text{yr.}$, respectively. This corresponds to approximately 0.5 kton/day, 0.9 kton/day and 0.3 kton/day and is the same order as the sedimentation simulated with Delft3D and the observed dredging volumes.

- Sea level rise leads to a reduction in deposition for the port basins Botlek and Amazonehaven, whereas an increase is observed for the Waalhaven. This behaviour is similar to the simulated Delft3D influence of sea level rise.

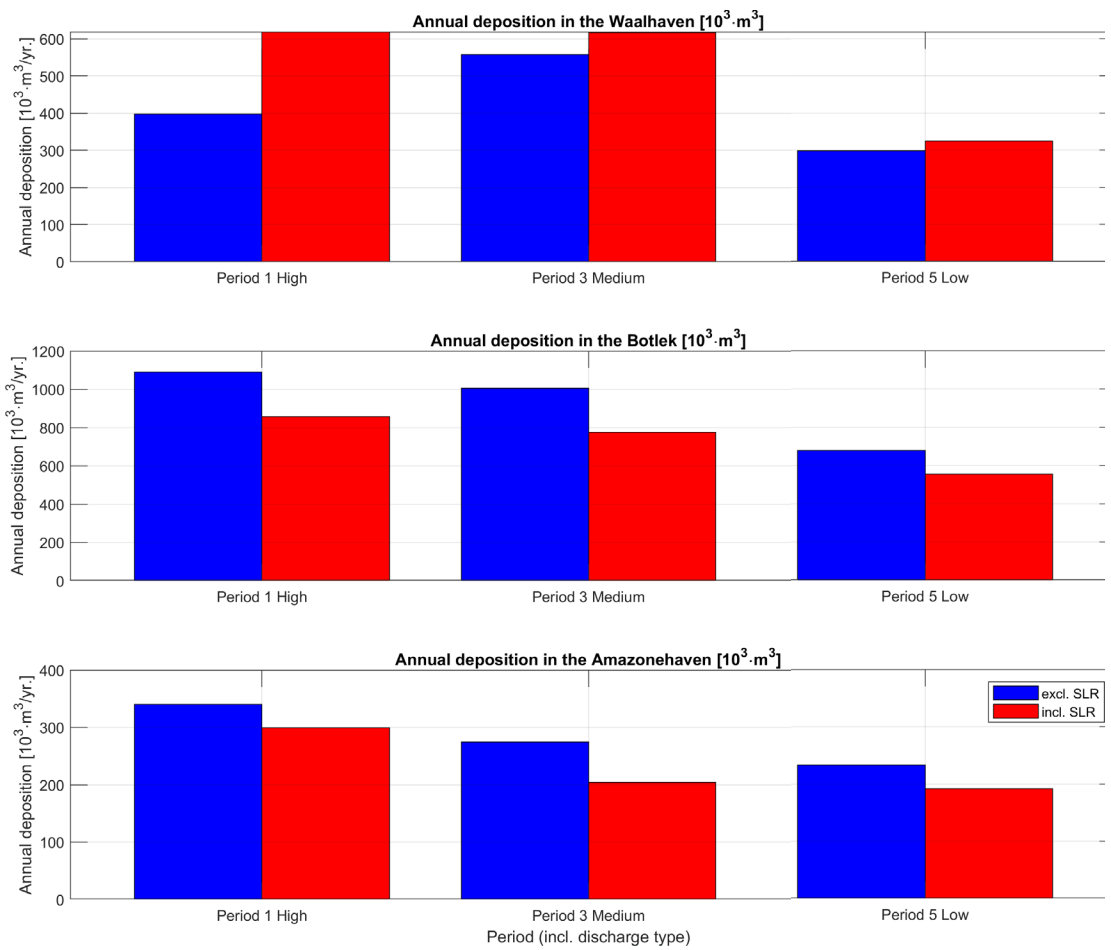


Figure 2-15 Annual deposition rates from SEDHAR, presented for the different port basins

3 WP2: Large scale STM and WID experiments

The sailing through mud (STM) and water injection dredging (WID) experiments were carried out in Deltares' Water Soil Flume (WSF)* and the Physical Laboratory (PL)*. Two MSc students, Aditya Pavan Kumar Goda (STM) and Sebastiaan Ma (WID), carried out the experiments and performed the reporting part of this work package. The two MSc graduations studies were supervised by Deltares and TU Delft personnel. A timeline of the experimental work package of TKI project DEL 126 PRISMA II can be seen in Figure 3.1.

*<https://www.deltares.nl/en/facilities/water-soil-flume/>

*<https://www.deltares.nl/en/facilities/physical-laboratory/>

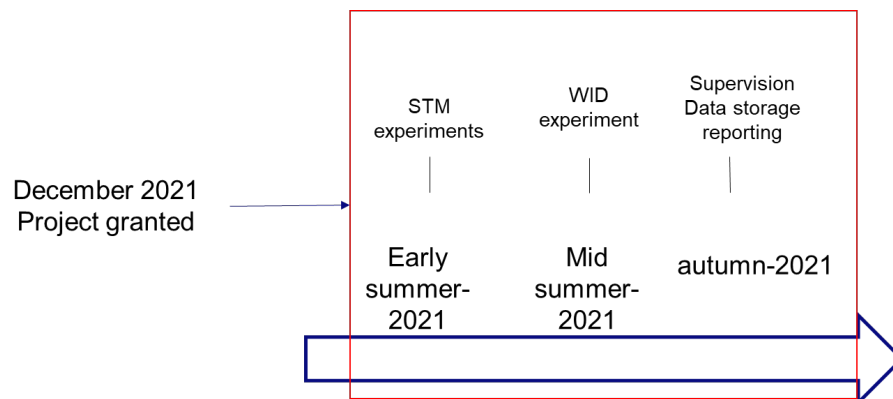


Figure 3.1: Timeline experimental work package of TKI project DEL 126 PRISMA II.

3.1 Sailing Through Mud experiments

3.1.1 Summary

The STM experiments for TKI project DEL 126 PRISMA II were carried out and analysed by Aditya Pavan Kumar Goda between 2021-2022. The following section contains the summary of his thesis (Goda, A. 2021). Data from the experiment and scripts can be found on the Deltares p-drive for TKI-Prisma2.

Thesis committee:

- Dr.ir. G.H. Keetels, TU Delft, chair
- Dr.ir. A.M. Talmon, TU Delft/Deltares
- Dr. Alex Kirichek, TU Delft
- MSc. Stefano Lovato, TU Delft
- Dr. ir. L. de Wit, Deltares

Ships are considered the best mode of transport throughout human history. The demand of goods transportation across the world increased exponentially over the past few decades. Therefore, ship size is increasing, which demands better infrastructure at ports and harbours. When a ship reaches the shore, the water depth reduces which reduces the under-keel clearance as well. The ship keel clearance influences the manoeuvrability of the sailing ship. Scientists and engineers are keenly studying the impact of very low under keel clearance and defining nautical bottom. In this thesis project, the link between fluid mud rheology and density was investigated. The exponential relation between bulk density and yield stress necessitates the direct measurement of rheology for navigability. It was confirmed that the yield strength increases exponentially with the density of the fluid mud. However, at higher densities of mud,

significant thixotropy is observed. Besides, the Power-law relations were found for the relation with volumetric concentration, for yield stress in agreement with fractal dimension theory. Second, quantification of the thixotropy effect of fluid mud is conducted to justify the importance of the time-dependency effect in the rheological modelling. We found that an unremoulded fluid mud has high thixotropy even at high shear rates. However, diluted and remoulded fluid mud at high shear rates found a negligible thixotropy effect. We also observed that Houska's modelling curve agrees well with the flow curve of fluid mud at high shear rates and integrates the thixotropy into the modelling. Third, the total resistance of a plate moving through fluid mud is measured and compared to the frictional forces calculated using the available analytical formulas of a plate moving in Bingham fluids and Power-law fluids. The moving plate is an abstraction of a vessel's keel sailing through the fluid mud. We found that the total resistance of the plate moved in fluid mud at low velocity agrees with the frictional force of a plate moved in Bingham fluids. As the velocity increases, the stagnation pressure becomes significant, and the deviation of the total resistance of the plate and frictional force of a plate increases. Thus, to estimate the total resistance of a plate moved in mud, normal forces (stagnation pressure) and flow circulations at edges should be investigated because these need to be subtracted. The experimental data in this thesis are made resourceful to help researchers validate their Computational fluid dynamics (CFD) models in the application of sailing through the mud.

3.1.2 Methods

The methods for the STM experiment consisted of two parts: 1) characterization of fluid mud in the Physical Laboratory and 2) Towing experiment of a wooden plate though fluid mud in the water Soil Flume (WSF). The material that was analysed for the characterization originated from Calandkanaal, Beerkanaal and 8^e Petroleumhaven, see Figure 3.2. The material that was used for the towing experiments originated from the Calandkanaal.

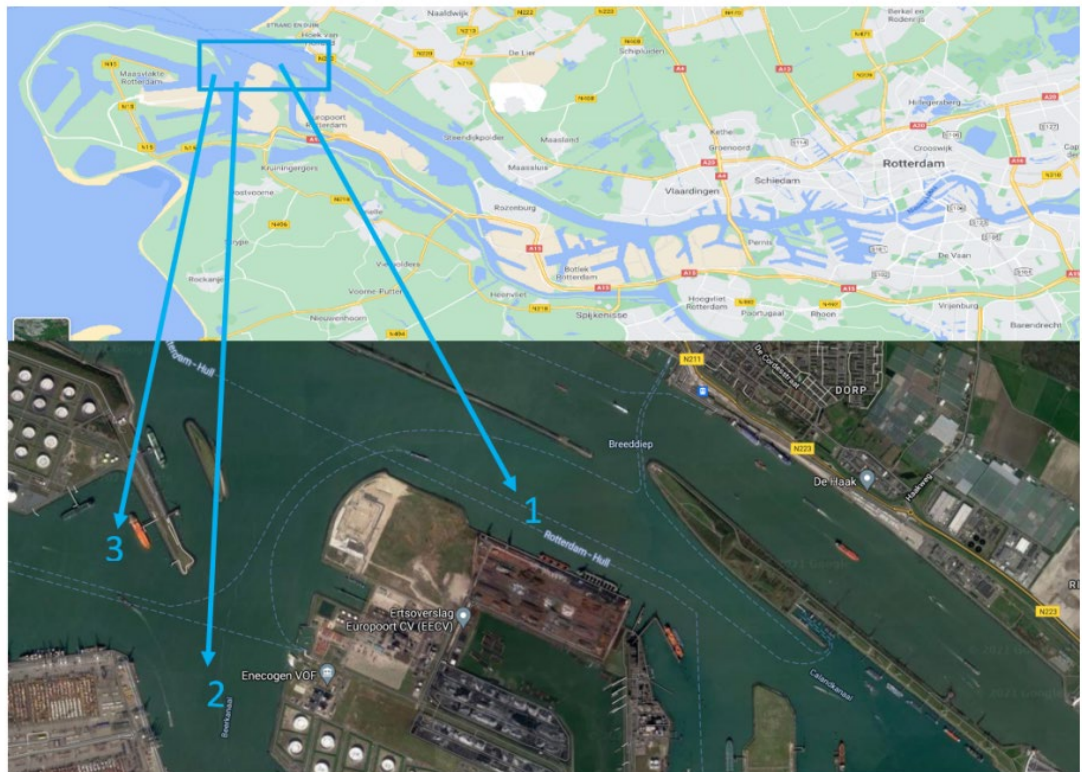


Figure 3.2: Calandkanaal (1), Beerkanaal (2) and 8^e Petroleumhaven (3).

3.1.2.1 Characterization of fluid mud in the PL

We used a FANN 286 Rheometer and a Thermo Scientific HAAKE Rheometer for rheology measurement, see Figure 3.3. We used bob, vane, groove bob, parallel plate, and double gap

bob-cup geometries for rheological protocols. Other soil properties were measured using DMA-35 manufactured by Anton Paar (for density) and an oven (for concentration, soil content and water content).



Figure 3.3: Thermo Scientific HAAKE Rheometer

3.1.2.2 Towing experiment in the WSF

For the towing experiment an abstraction of a vessel, a wooden plate, was towed through three different dilutions in the WSF with different velocities (0 m/s -- 1 m/s), see Figure 3.4. The force on the plate was measured with a load cell that was connected to the wooden plate.

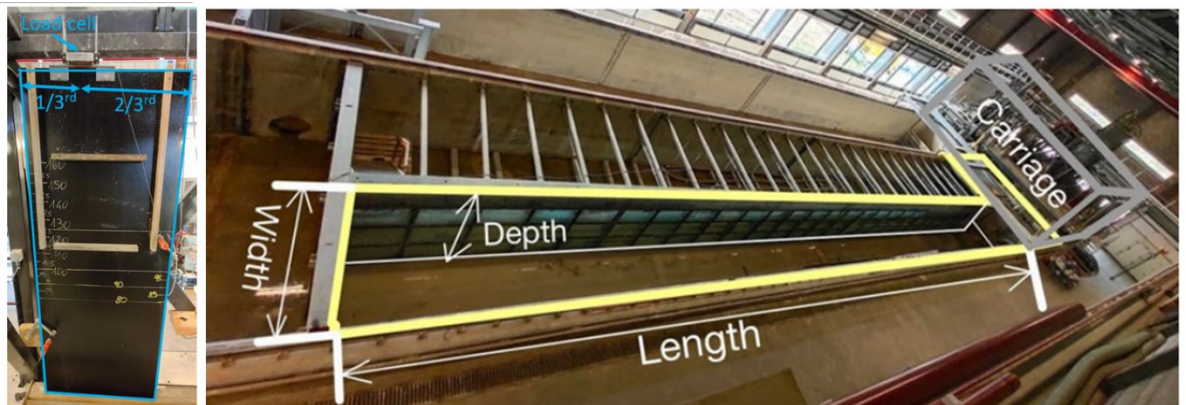


Figure 3.4: Left: plate with dimension 0.8 m length, 1 m submerged depth in fluid mud and a thickness of 1.2 cm. The force meter was located at 1/3 length from the leading edge. Right: WSF with dimensions 31 m length, 2.5 m depth, and 2.5 m depth in this configuration.

Another device has also been used for the towing experiment in the WSF: the CUX sampler provided by the Port of Hamburg, see Figure 3.5. There were some difficulties with obtaining repeatable and reliable force signals so therefore the analysis of Pavan Goda focussed on the wooden plate geometry. The CUX measurement data and an overview presentation of the CUX measurements is shared with the Port of Hamburg.



Figure 3.5 CUX sampler from Port of Hamburg

3.1.3 Key findings

3.1.3.1 Objective 1: To find the link between sediment properties (density and salinity) and rheological properties.

From three locations in the Port of Rotterdam fluid mud sediment samples were collected and diluted with seawater and freshwater to analyse changes in rheological parameters as a function of density and salinity. This was done to target specific densities for the towing experiment (objective 3). Diluting material with fresh water is not representative for natural conditions in the Port of Rotterdam. However, if salinity does not change rheology, fresh water dilutions can be used to associate density and sailing velocity to the resistance of a ship sailing through fluid mud (objective 3). The relation between concentration, solid content, water content, Bingham yield stress, static yield stress, fluidic yield stress, and dynamic yield stress for three sites in the Port of Rotterdam can be found in Table 4.3 of MSc thesis of Aditya Pavan Kumar Goda. Key findings of objective 1 were:

- It was found that rheological strength parameters (yield stresses) increase exponentially with density, see Figure 3.6. Moreover, in terms of rheological behaviour, fluid mud from 8^e Petroleumhaven and Calandkanaal are comparable.
- Yet, rheological parameters of fluid mud from Beerkanaal change less with density (smaller base in the exponential relationship).
- In addition, salinity does not influence the density- yield stress relation.

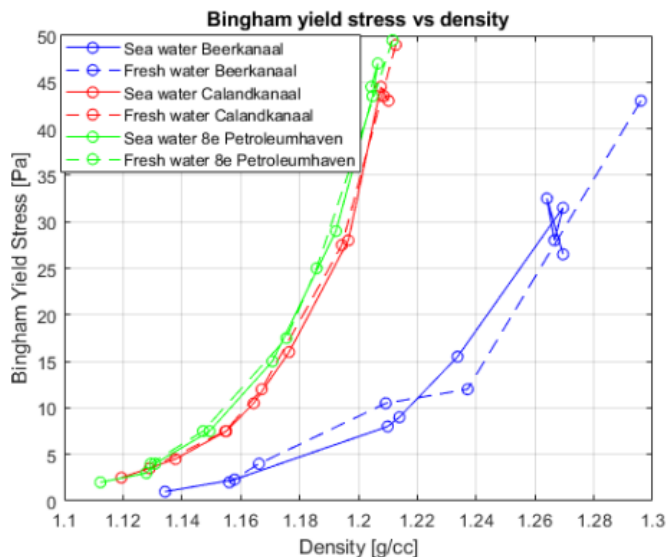


Figure 3.6: Relationship between density and Bingham yield stress for mud from different locations in the Port of Rotterdam. Variance of densities was acquired by dilution high density sampled per location. Density of seawater used for sea water dilution was 1025 kg/m^3 . For fresh water dilutions, a water density of 1000 kg/m^3 was used.

3.1.3.2 Objective 2: To find how thixotropy of fluid mud can be quantified considering the non-Newtonian rheological modelling.

Fluid mud can gain strength after a period of recovery. The effect of time-dependency is quantified by measuring the flow curve of sediment sheared ramping up to maximum disturbance (high shear) and subsequently, sheared ramping down to zero disturbance. This is called a hysteresis loop, see Figure 3.7 for an example of the originally sampled mud from the Calandkanaal for the towing experiments. Key findings of objective 2 were:

- Thixotropy is quantified for originally sampled mud from the Calandkanaal and dilutions of this original material from the port that was used for the towing experiments, see objective 3.
- Time dependency for rheology can be modelled using the Houska model, see Figure 3.7 and see Houska formulation below. Here, τ is the shear stress, τ_∞ is the yield stress of totally destructed fluid, λ the is structural parameter, τ_0 is the yield stress of fully structured fluid, μ_∞ is the viscosity of totally destructed fluid, c is the maximum increment of viscosity, $\dot{\gamma}$ is the shear rate, n is the power law index. The Houska model consists of a simple non-Newtonian equation of state for base condition (fully remoulded) plus a part that describes structure dependent rheology. Curve fitting parameters for in-situ Calandkanaal, and the three towing structure-dependent experiments are given in Table 5.3 in the MSc thesis of Aditya Pavan Kumar Goda.

$$\tau = \tau_\infty + \lambda(\tau_0 - \tau_\infty) + (\mu_\infty + \lambda c)\dot{\gamma}^n \quad (14)$$

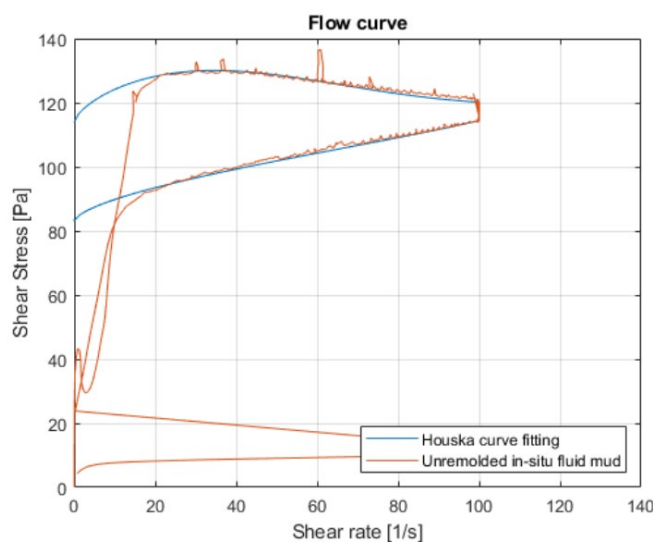


Figure 3.7: Hysteresis loop and modelled Houska curve for in situ Calandkanaal mud. Dilutions of this mud was used for towing experiments, see section below.

3.1.3.3 Objective 3: To relate existing analytical formulas for non-Newtonian fluids and how they can be used for estimating the plate resistance measured in the flume experiments.

Since fluid mud shows non-Newtonian rheological behaviour, computing frictional forces on ships sailing through fluid mud is not straightforward. For this objective, we measured frictional forces acting on an abstraction of a sailing vessel, a wooden plate. The wooden plate moved through three dilutions of Calandkanaal fluid mud (Bingham yield stress 9, 17, 21 Pa) with varying velocities (0.25-1 m/s), see Figure 3.8. Key findings were:

- We found that the total resistance of the plate divided by the plate surface area extrapolated to zero velocity agrees with the Bingham yield stress of the mud.

- As the velocity increases, the stagnation pressure becomes significant, and the deviation of the total force (resistance and frictional force) increases. Thus, to estimate the total resistance of a plate moved in mud, normal forces (stagnation pressure) and flow circulations at edges should be investigated because these need to be subtracted.

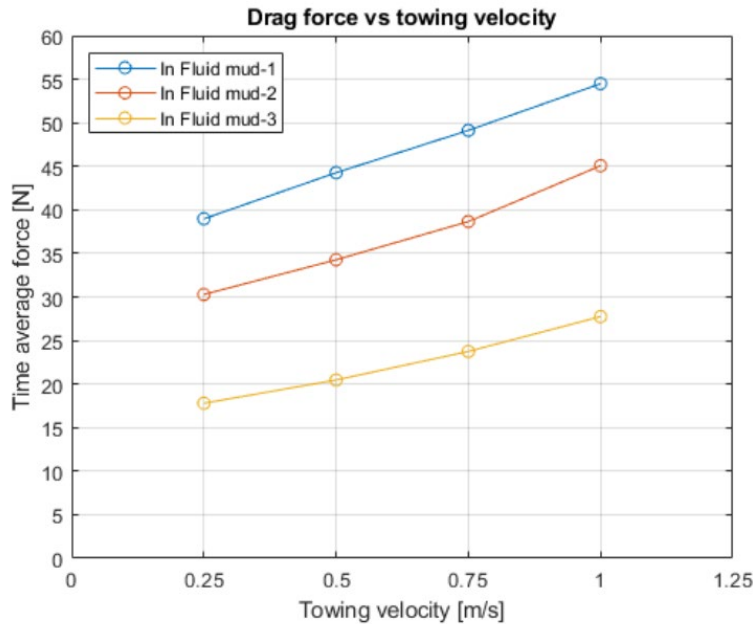


Figure 3.8: Time average of the force on the plate as function of towing velocity in three dilutions of fluid mud from the Calandkanaal.

3.2 Water Injection Dredging experiments

3.2.1 Summary

The WID experiments for TKI project DEL 126 PRISMA II research were carried out and analysed by Sebastiaan Ma between 2021-2022 (Ma 2022). The following section contains the summary of his thesis.

Thesis committee:

- Prof. dr. ir. C. van Rhee, TU Delft, chair
- Dr. A. Kirichek, TU Delft
- Dr. C. Chassagne, TU Delft
- Dr. ir. L. de Wit, Deltares
- Dr. ir. A. M. Talmon, TU Delft/Deltares, daily supervisor

Company supervisors:

- E. Hupkes Port of Rotterdam
- Ir. J. Smits Port of Rotterdam

The Port of Rotterdam experiences large amounts of siltation from the upstream rivers in its basins and access channels every year. Furthermore, container vessels increase in size every decade and therefore require a larger navigational depth. These two factors cause the yearly amount of dredged material to increase. Currently, mainly trailing suction hopper dredgers are used to remove the large amounts of sediment, but these vessels come with high costs and operational time. A more time and cost-efficient dredging method is therefore desired.

A potential solution to the increasing problems of costs and operational time by dredgers is the technique of water injection dredging. In order to make this technique as efficient and effective as possible, this study conducted experiments to measure and analyse flow and sediment properties for different parameter settings of water injection dredging and optimize the dredging technique on mud from the Port of Rotterdam. Large-scale experiments have been conducted in the water-soil flume (WSF) of Deltares, where a jet bar was trailed (or run) over a bed 27 meters long and 0.5 meters deep of port mud while injecting it multiple times with water. The traverse velocity, nozzle pressure, nozzle diameter and stand-off distance (SOD) were varied. The created density current flowed towards a measuring frame where the flow velocity and density at different heights were measured in time. This results in flow velocity and density profiles of the density current. The intrusion depth by the jets, the jet settings, density of the current behind the jet bar and the rheology of the mud were measured as well. Through this data, the production rate and behaviour of the density current are determined and described as a function of the jet settings.

A positive relationship is observed between the production rate and jet momentum when considering the data of the intrusion depth and analysed samples of the bed, together with the data of the measured jet settings. The production can be related linearly with the jet momentum by means of the Vlasblom equation combined with a non-dimensionless empirical fitting parameter per run per traverse velocity. Remarkable is the increasing intrusion depth of the jets with ascending runs while the jet parameter settings stay the same. The data shows that the difference between the mass flux by the density current and the mass flux stirred up by the jets, increases between runs when an increased intrusion depth between those runs is observed as well. Here, the sediment concentration of an undisturbed bed was assumed. This indicates that the volume penetrated by the jets contained a smaller amount of sediment than was assumed initially, thus is disturbed by the previous run and therefore decreases in strength. This decrease in strength results in a larger intrusion depth during the run itself in comparison to the previous run. Furthermore, the analysis on the production rates also shows that the density current transports more sediment when a high jet momentum is applied. A super-critical density current ($Fr^2 > 1$) was recorded for jet momentum per width values that exceeded 500 N/m. For a supercritical density current, relatively more horizontal momentum at the ramp was measured as well. Next to the jet momentum, the influence of the SOD of the jets was analysed by comparing runs with a SOD to runs without a SOD but with similar remaining jetting parameter settings. When a SOD is applied, the jet pressure applied to the bed is outside the flow development region and therefore the jet pressure decreases with distance from the jet nozzle. The data shows that the mass of sediment stirred up by the jets, for a SOD of 300 mm, is lower in comparison to a SOD of 0 mm. The density current transports relatively more sediment, however, when a SOD of 300 mm is applied. This is attributed to the observation that sediment is stirred up higher in the water column and therefore has more time to settle, in combination with high flow velocities also measured at these higher positions in the water column and entrainment. So, if a large amount of sediment needs to be stirred up, and therefore a large intrusion depth is required, no SOD should be applied and when large horizontal transport by the density current is desired, a SOD outside the flow development region of the jets should be used.

3.2.2 Methods

The large-scale WID tests were performed in the WSF to find the optimal parameter setting of water injection dredging to maximize production. Water injection dredging was performed by trailing a jet bar over the flume that injects water through nozzles located in the jet bar into a 27 m long and 0.5 m deep layer of mud from the Port of Rotterdam, see Figure 3.9. Including a test run, seven tests were performed. In these tests the traverse velocity, nozzle pressure, nozzle diameter, and standoff distance (SOD_b) were varied. The SOD_b is the distance between the sediment bed and the nozzles in the jet bar. Water injection created a density current that was analysed at a measurement frame at the end of the flume, this was called the ramp, see

Figure 3.9. Flow velocity and density variation over depth and time was measured at the measurement frame with conductivity meters and the directly behind the jet bar. The intrusion depth by the jets, the jet settings, density of the current behind the jet bar, and the rheology of the mud were measured as well. Bed level changes were measured with a disk attached to a rope, since the echo sounder was unable to record the bed changes correctly due to all kinds of reflections from the hard walls and floor in the flume interfering with the signal.

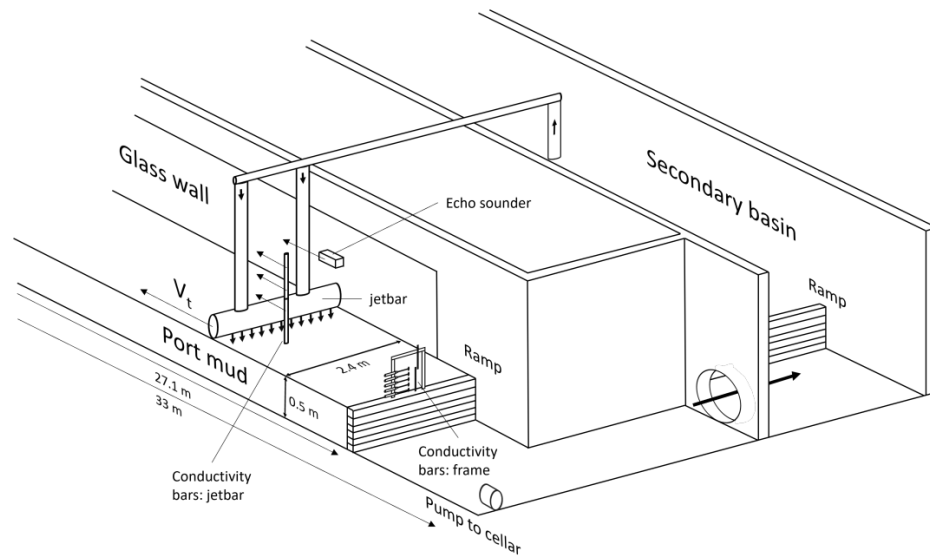


Figure 3.9: Schematization of the WID experimental set-up in the WSF.

3.2.3 Key findings

3.2.3.1 Objective 1: To measure and analyse flow and sediment properties during the experiments in the watersoil flume for different parameter settings of water injection dredging.

In order to find optimal settings for WID (objective 2), first, the following flow and sediment properties were analyzed: the bi-directional flow profile, suspended sediment concentration profile, bathymetry before and after runs over the whole length of the flume and rheological properties of the bed before the start of the experiments. See chapter 6 of the MSc thesis of Sebastiaan Ma for quantifications of all tests. Key finding were:

- Flow velocities of the density current range between 0.1 and 0.6m/s at the ramp.
- The density current reaches values up to 1.15 g/cm³ at the ramp.
- The height of the density current was between 0.1 m and 0.4 m.
- Mud with different strengths was tested. The range of Bingham yield stresses that was tested was between 80 Pa and 237 Pa.

See Figure 2.9 and Figure 2.10 for two examples of the measured density and velocity profiles in the fluid mud layer which are used for CFD model validation.

For some experimental combinations of jet pressure, nozzle diameter, SOD, trail speed and mud-bed-strength no horizontal transport was taking place. For those cases, a fluidized mud layer was generated which was more or less stable showing very low velocities <0.1 m/s. This happened for tests 3,4, 5. Test 6 investigated the influence of SOD and gave a non-flowing fluid mud layer for the one run with low SOD and a moving fluid mud layer for the three runs with larger SOD. See Table 3-1 for the settings of those tests. These tests differ from tests 1 and 2 by their nozzle diameter. Tests 1 and 2 have a nozzle diameter of 35 mm, and tests 3-6 had a nozzle diameter of 20 mm.

3.2.3.2 Objective 2: To find the optimal parameter setting of water injection dredging to maximize production.

An overview of WID setting and resulting production is portrayed in Table 3-1. Key findings related to objective 2 were:

- A positive relation between the production rate and jet momentum was found. The mass of sediment stirred up by the jets can be related linearly to the jet momentum using the Vlasblom equation where a non-dimensionless empirical fitting parameter is iterated per run per traverse velocity vt . This relation can be used to apply the optimal jet settings for the desired production rate.
- An interesting observation is that subsequent WID runs on the same bed give extra jet penetration compared to the previous run with similar settings. It is not fully understood yet what causes this observed phenomenon.
- Supercritical flow (Densimetric Froude number >1) of the density current improves the efficiency of the density current leading to more horizontal transport. Supercritical flow is reached in the experiments at jet momentum per width > 500 N/m.
- If a large intrusion depth is required, no SOD should be applied and when large horizontal transport by the density current is desired, a SOD outside the flow development region of the jets (tested is $\sim 12x$ nozzle diameter) should be used.

Table 3-1: Settings and test results of all tests. Here, v_t is the trailing velocity, D_n is the nozzle diameter, p_j is the jet nozzle pressure, SOD_r is distance between the nozzle and the ramp, SOD_b is the distance between the nozzle and the sediment bed, τ_B is the Bingham yield stress, I_j is the jet momentum per unit width, $s_{av,intr}$ is the average representative intrusion depth, production is the initial production at the jet bar.

		v_t [m/s]	D_n [mm]	p_j [bar]	SOD_r [mm]	SOD_b [mm]	τ_B [Pa]	I_j [N/m]	$s_{av,intr}$ [m]	Production [kg/s]
Trial week	Run 1	0.25	20	0.54	10	-	109	192.22	0.03	9.39
	Run 2	0.25	20	1.07	10	-	109	426.04	0.06	18.87
	Run 3	0.25	20	1.06	10	-	109	391.84	0.06	18.87
	Run 4	0.25	30	0.49	10	-	109	345.46	0.09	28.31
	Run 5	0.25	30	1.03	10	-	109	863.08	0.11	34.57
Test 1	Run 1	0.25	35	0.51	10	-60	118.2	566.3	0.08	20.16
	Run 2	0.25	35	0.52	10	-60	118.2	575.4	0.17	44.35
	Run 3	0.25	35	0.53	50	10	118.2	579.7	0.24	64.51
Test 2	Run 1	0.40	35	0.51	70	70	80.15	559.7	0.21	85.88
	Run 2	0.40	35	0.50	70	140	80.15	560.2	0.16	65.43
Test 3	Run 1	0.40	20	1.06	10	-10	156	424.6	0.06	25.48
	Run 2	0.40	20	1.05	10	0	156	415.8	0.10	44.96
	Run 3	0.40	20	1.03	10	-30	156	423.8	0.18	79.42
	Run 4	0.40	20	1.02	60	60	156	423.5	0.13	58.44
Test 4	Run 1	0.25	20	1.02	10	-60	237.2	410.5	0.06	19.53
	Run 2	0.25	20	1.04	10	-50	237.2	416.4	0.14	44.20
	Run 3	0.25	20	1.02	10	20	237.2	410.6	0.17	52.43
Test 5	Run 1	0.25	20	0.50	10	-10	132.7	217.1	0.05	12.10
	Run 2	0.25	20	0.51	10	-20	132.7	219.7	0.07	18.82
	Run 3	0.25	20	0.51	10	-50	132.7	223.2	0.06	16.13
	Run 4	0.25	20	0.50	60	10	132.7	214.2	0.10	26.88
Test 6	Run 1	0.40	20	1.00	300	220	112.2	399.6	0.05	13.32
	Run 2	0.40	20	1.06	300	230	112.2	433.5	0.08	19.98
	Run 3	0.40	20	1.06	60	-40	112.2	446.2	0.22	57.28
	Run 4	0.40	20	1.04	300	260	112.2	458.7	0.16	41.29

3.3 Recommendations on future experiments

The majority of the experiments conducted for WP2 were performed in two research facilities: WSF (water-soil flume) and FL (Fysisch Laboratorium: Physical Laboratorium). Based on these experiments some recommendations for future experiments of similar scope and topic are discussed.

3.3.1 Recommendation related to STM

- One of the major issues during the STM experiments was the unreliability of the force meters of the CUX-sampler. The CUX-sampler is a device that can measure drag forces and is used also in other surveys of sediment beds in ports and waterways. Some instrumental drift of the force meters attached to the wings was observed. A solution was using a wooden plate with an attached force meter. Yet, for higher towing velocities this method also have limitations, see key findings of STM.
- Local homogenizing in the WSF is very well possible with the propeller-mixer available at Deltares. In case of more severe inhomogeneities it is recommended to pump the mud from one side of the flume towards the other part being a much faster and cost-effective method.

3.3.2 Recommendation related to WID

- Extracting samples from the density current during WID experiments did not work because of unsuitable tubes and pumps. Therefore, rheology measurement from the density current could not be performed. An investment into in-situ rheology

measurement at different depths would improve the quality of the data for WID experiments in the WSF and is useful for CFD modelling of density currents.

- It turned out to be difficult to determine the exact WID production (amount of sediment loosened and transported away by the WID jet bar) in the experiment and the experimental results indicate that during WID a layer of mud may be weakened but not transported. It is recommended to add bulk density and strength measurements in the sediment bed to be able to track the jet penetration and soil weakening during the experiment in more detail. Also, it is recommended to make very exact bathymetry measurements in between WID trails, perhaps via a side-glass wall or by removing all water in between subsequent WID trails as now either by the echosounder or by the disk measurements there remains some uncertainty in the exact amount of sediment removed by each WID trail.

3.3.3 Recommendation related to logistics

Large quantities of mud were used during WP2: 194 m³ of mud was used per STM test; 33 m³ of mud was used per WID test. Therefore, carefully planned and executed logistics were essential for this project. First, the material was dredged from the top sediment layer at the Calandkanaal in the Port of Rotterdam by a hopper dredger from the Port of Rotterdam. The vessel mixed the water with the mud at the Scheurhaven. Thereafter, the mud was pumped into a truck and transported to Deltares. At Deltares the mud was distributed equally into the WSF, see Figure 3.10. Due to time constraints a low number of in-between pause days were planned but given the complexity and scale of logistics of these tests there should be enough contingency time in the planning to allow for a doubling in transportation time from one day to two days for every test. Related to the large quantities, some logistical problems arose, which will be elaborated on in Table 3-2.

Table 3-2: Encountered logistical problem, consequence and recommended solution.

Encountered problem	Consequence	Recommendation
Broken pumps due to metal pieces in dredged material	Pumps required reparations, tests were delayed.	Having multiple pumping trucks available + make sure that during dredging the hopper is completely clean without metal pieces from previous dredging works which in this experiment was ensured and emphasised towards the captain of the dredging vessel only for the last couple of days
Having only one pumping truck available	Pumping into the truck and into the WSF was laborious and time consuming	Having multiple pumping trucks available
At the moment of disposal of mud prior to STM experiments, it was uncertain how much water was needed to dilute the mud to the correct shear strength values.	Too much water was pumped into WSF so shear strength values were lower than initially planned	Have density versus shear strength relation available prior to pumping water-mud ratios into WSF, so that correct quantities of mud and water are used.



(a) Crane loading the mud into the hopper.



(b) Mud inside the hopper after dredging.



(c) Pumping the mud from the hopper into the truck for transport to Deltares.



(d) Pumping the mud from the truck into the flume.

Figure 3.10: Transportation of mud from the Port of Rotterdam to Deltares.

4 WP3: Data science for optimizing dredging

In WP3 an intern from WUR, Cristina Panez has carried out data analyses for optimizing dredging under supervision of G. Santinelli, data science and water quality advisor/researcher at Deltares. This research aims to gain insight into ways to increase the effectiveness of maintenance dredging activities in the Port of Rotterdam. Additionally, this work aims at identifying the difference in the dredging performance with different types of sediments. This resulted in a data-driven decision support tool for Port authorities.

The dredging efficiency concept is clarified together with dredging field experts and researchers to find a way to establish this term within this study. Two areas of the port of Rotterdam with sandy and silty sediment material types were studied, namely Maassluis and the Botlek. Each area presents two cases. The methodology performed in this study was based on the availability of the data and dredging experience. Each case provides dredging on board data and bathymetric survey data before and after the dredging activity. The bathymetric survey, together with the Nautical Guaranteed Depth (NGD), was used to identify areas that comply with the NGD before and after the dredging activity. Four categories were assigned at each location for a specific survey cover area and along the trajectory, see Figure 4.1. The percentages of each category were calculated.

yesyes	both measurements comply with NGD
noyes	first measurement does not meet and second does comply with NGD
yesno	first measurement meets NGD and the second does not
nono	both measurements do not meet NGD

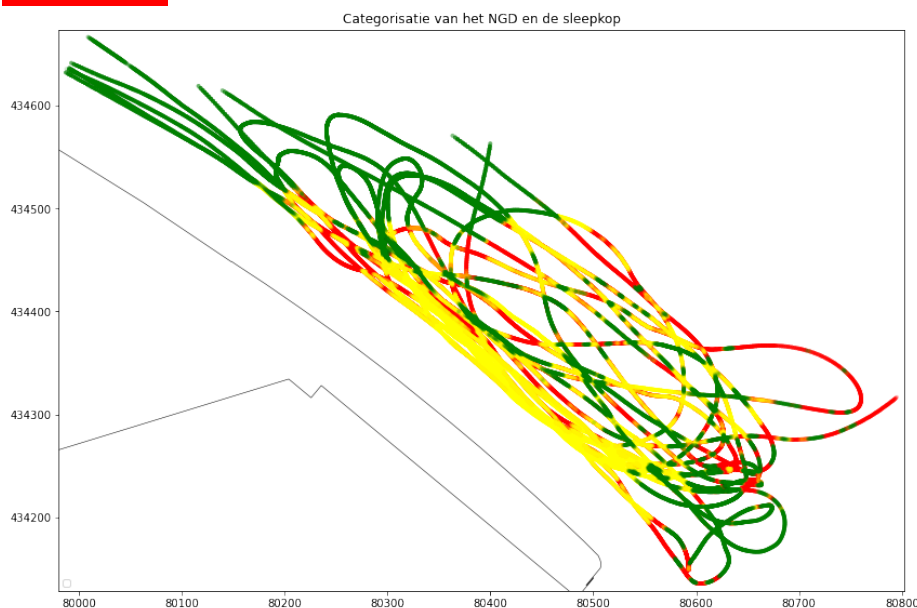


Figure 4.1 Example of the four NGD categories for a dredging trip in Botlek area

The results show that more than 70% of the locations along the dredging trajectory were already complying with the NGD before and after in Maassluis and Botlek. According to the Port of Rotterdam, this is the so-called “preventive dredging”. In Maassluis cases (mostly sandy channel bed), less than 5% of locations along the dredging trajectories were categorized as not complying before and after the dredging activity. This number is much lower than in the two Botlek cases (mostly silty channel) where it was found to be 13 and 26%.

Statistical summaries per category were performed to identify data trends in the four cases. A correlation heatmap, see Figure 4.2, was used to identify correlations between the survey data and the on-board data along their trajectories. Unfortunately, no striking correlations were found between on-board and bathymetric data.

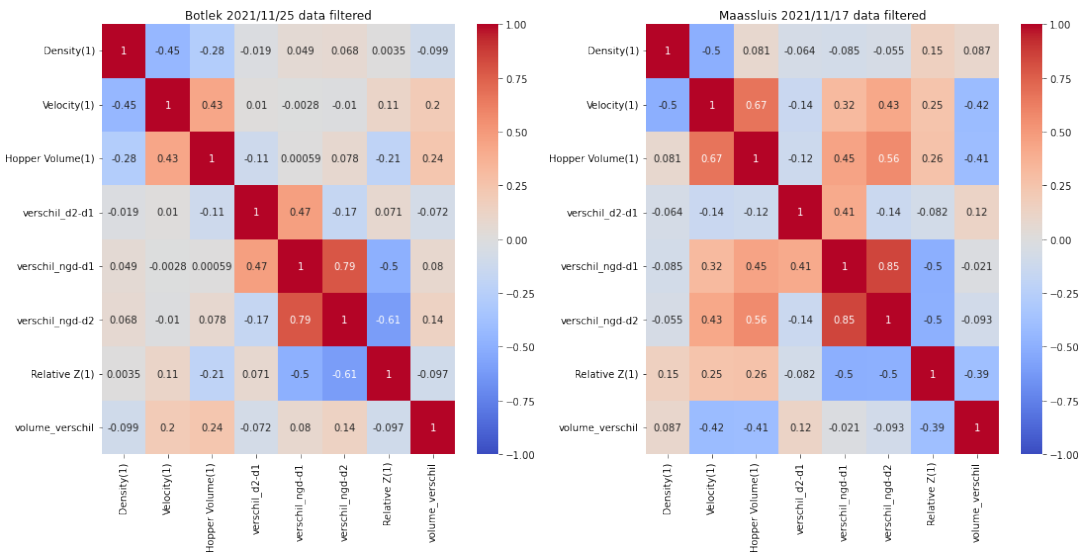


Figure 4.2 Two examples of correlation heatmaps for a Botlek and Maassluis trip

The analysis in Figure 4.3 shows interesting features. Highest deepening is found for spots which did not comply before and did comply after dredging. That is expected. But interesting to see is that the deepening for spots which did not comply before and after dredging is very similar for 3 out of these 4 trips to the deepening for spots which did comply before and after. And locations that did not comply with NGD (before and after dredging) presented a high density of sediment-water mixture inside the suction pipe in the Botlek and Maassluis cases, see Figure 4.3 (right). Apparently, at spots which do not comply before and after dredging the dredging efficiency is not the problem but simply more dredging trails on those spots are needed.

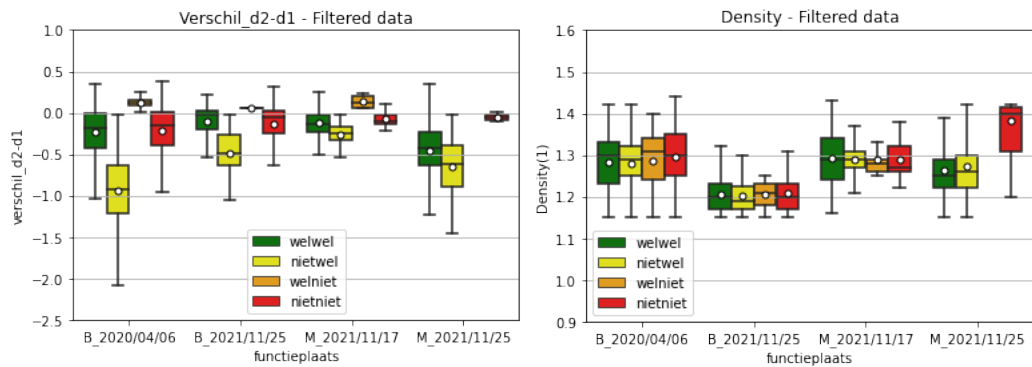


Figure 4.3 Two examples of using the NGD classification to analyse other parameters: difference in bathymetry before and after dredging (left) and mixture density in TSHD suction pipe (right)

In a follow-up the developed data science tools can be applied to more trips and see what trends are visible and how this can be used to optimize application of hopper dredging in sandy and muddy areas.

5 Overview detail reports and datasets TKI Prisma2

The following detail reports and memos are available from TKI Prisma 2:

- Memo field measurements of WID turbidity (Keulen 2021)
- Memo influence SLR on sedimentation PoR (Jaksic et al. 2022)
- COSUMO coupling tool D3D-CFD for WID density current (Verbruggen, de Wit 2022)
- Overview report summarizing all activities of TKI Prisma 2 (present report)

The following data sets are available from TKI Prisma 2:

- Data set Sailing Through Mud experiments water-soil flume
- Data set WID experiments water-soil flume

The following student graduation reports are available from TKI Prisma 2:

- MSc report TU Delft: A. Goda 2021 Rheological and plate's hydrodynamic resistance in fluid mud measurements for the nautical bottom applications
<https://repository.tudelft.nl/islandora/object/uuid%3Adb54cf8e-53ca-4387-94d5-1e0a3945df35?collection=education>
- MSc report TU Delft: E. ten Brummelhuis 2021 Modelling of high concentration fluid mud water injection dredging density currents
<https://repository.tudelft.nl/islandora/object/uuid%3Ae4b50eee-adce-4847-9ed5-4528b58658c0?collection=education>
- MSc report TU Delft: S. Ma 2022 Laboratory study on the efficiency of water injection dredging: An analysis on the influence of different dredge settings on the density current and production
rate <https://repository.tudelft.nl/islandora/object/uuid%3Ac446d61a-9073-438d-aa1e-1f3c22045bd0>
- MSc internship report WUR: C.C. Panez 2022 Data-driven assessment of port maintenance efficiency: Case study Port of Rotterdam

The following papers using data and results from TKI Prisma 2 are available:

- Conference paper: Wit, L. de, E. ten Brummelhuis & A. Talmon (2022), 3D CFD modelling of water injection dredging including mud rheology, Proceedings of the 23th World Dredging Conference WODCON XXIII, Copenhagen, Denmark
- Journal publication: S.Lovato, A.Kirichek, S.L.Toxopeus, J.W.Settels, G.H.Keetels (2022), Validation of the resistance of a plate moving through mud: CFD modelling and towing tank experiments, Ocean Engineering, volume 258,
<https://doi.org/10.1016/j.oceaneng.2022.111632>

References

- Brummelhuis, E. ten, 2021, MSc thesis, Modelling of high concentration fluid mud water injection dredging density currents
<https://repository.tudelft.nl/islandora/object/uuid%3Ae4b50eee-adce-4847-9ed5-4528b58658c0?collection=education> , TU Delft MSc graduation report
- Cronin K, Huismans Y and van Kessel T. 2019. Local mud dynamics and sedimentation around the Maasmond. Final report. Deltares, 11202804-000-ZKS-0003
- Eysink, W.D. (2004). SILTHAR version 4.2 – A mathematical program for the computation of siltation in harbour basins. WL | Delft Hydraulics.
- Goda, A. 2021 Rheological and plate's hydrodynamic resistance in fluid mud measurements for the nautical bottom applications
<https://repository.tudelft.nl/islandora/object/uuid%3Adb54cf8e-53ca-4387-94d5-1e0a3945df35?collection=education> ,TU Delft MSc graduation report
- Hendriks E. and Schuurman F. 2017. Modelling alternatieve loswal locaties, Final report, Deltares, 1230860-000-ZKS-0008, 4 oktober 2017.
- Jaksic L., Scheel F., Wit L. de , Boer W. de, Kessel T. van 2022. Impact SLR on sedimentation PoR. Deltares memo 11206938-002-ZKS-0001, 2 november 2022
- Keulen D. van 2021. Memo silt profiles WID. Deltares memo 11206938-002-ZKS-0001, 14 july 2021
- Kirichek A. 2016. Rheological characteristics of fluid mud for ports and waterways. Internal report, the Port of Rotterdam.
- Kirichek A, Rutgers R, Wensveen M and Van Hassent. 2017. Sediment management in the Port of Rotterdam. In: Proceedings of the 10th Rostocker Baggergutseminar; 11-12 September 2017; Rostock.
- Kirichek A, Chassagne C, Winterwerp H and Vellinga T. 2018. How navigable are fluid mud layers? Terra et Aqua, 151:6-18.
- Kirichek A and Rutgers R. 2020. Monitoring of settling and consolidation of mud after water injection dredging in the Calandkanaal. Terra et Aqua, 160:16-26
- Kirichek A, Shakeel A and Chassagne C. 2020. Using in situ density and strength measurements for sediment maintenance in ports and waterways. J. Soils Sediments, 2546–2552. DOI: [10.1007/s11368-020-02581-8](https://doi.org/10.1007/s11368-020-02581-8).
- Kirichek, A., Cronin, K., de Wit, L., Meshkati, E., van Keulen, D., & Terwindt, J. (2021a). PRISMA I: Final report. Deltares, 11203928-000-ZKS-0004_v0.1, 12 August 2021
- Kirichek, A., Cronin, K., de Wit, L., van Kessel, T., (2021b). Advances in Maintenance of Ports and Waterways: Water Injection Dredging. Sediment Transport - Recent Advances

Ma, S. 2022 Laboratory study on the efficiency of water injection dredging: An analysis on the influence of different dredge settings on the density current and production rate <https://repository.tudelft.nl/islandora/object/uuid%3Ac446d61a-9073-438d-aa1e-1f3c22045bd0> , TU Delft MSc graduation report

Panez, C.C. 2022 Data-driven assessment of port maintenance efficiency: Case study Port of Rotterdam, WUR MSc internship report

PIANC. 2013. Injection Dredging, Report 120, PIANC, Brussels.

PIANC. 2014. Harbour Approach Channels - Design Guidelines, Report 121, PIANC, Brussels.

Van Rijn, L.C. (2005). Principles of Sedimentation and Erosion Engineering in Rivers, Estuaries and Coastal Seas. Aqua publications, Blokzijl.

Verbruggen W., de Wit, L. 2022. Delft3D – COSUMO - CFD coupling for WID. Deltares pptx, 5 april 2022

Verhagen HJ. Water injection dredging. In: Proceedings of the 2nd International Conference Port Development and Coastal Environment (PDCE 2000); 5-7 June 2000, Varna, Bulgaria, 2000.

Wit, L. de, E. ten Brummelhuis & A. Talmon (2022), 3D CFD modelling of water injection dredging including mud rheology, Proceedings of the 23th World Dredging Conference WODCON XXIII, Copenhagen, Denmark

Wurpts R and Torn P. 2005. 15 Years' Experience with Fluid Mud: Definition of the Nautical Bottom with Rheological Parameters, Terra et Aqua, 99:22-32

Deltares is an independent institute for applied research in the field of water and subsurface. Throughout the world, we work on smart solutions for people, environment and society.

Deltares

www.deltares.nl